Study of the shrinking behaviour of PGL-3 droplets during glass-like ageing

Stoffers, Bart

Study of the shrinking behaviour of PGL-3 droplets during glass-like ageing

THESIS

submitted in partial fulfillment of the
requirements for the degree of

BACHELOR OF SCIENCE
in
PHYSICS

Author :	Bart Stoffers
Student ID :	274644
Supervisor :	Louise Jawerth
	(PhD student) Nathan van den Berg
Second corrector :	Martin van Hecke

Leiden, The Netherlands, December 4, 2025

Study of the shrinking behaviour of PGL-3 droplets during glass-like ageing

Bart Stoffers

Huygens-Kamerlingh Onnes Laboratory, Leiden University
P.O. Box 9500, 2300 RA Leiden, The Netherlands

December 4, 2025

Abstract

Biomolecular condensates are membrane-less compartments in cells, which are made up of proteins and nucleic acids, that exist through liquid-liquid phase separation. Research has shown that these condensates have time dependent material properties that change in a process called glass-like ageing. Understanding why and how these condensates age could lead to advancements in biochemistry, where non-functioning condensates have already been linked with neurodegenerative diseases. Investigating this ageing behaviour by looking at the changing properties could reveal insights in how these condensates work and why they undergo glass-like ageing. PGL-3 is such a protein that can be present in condensates which show glass-like ageing. However, PGL-3 droplets also shrink over time. In this research code is developed to investigate this shrinking behaviour of PGL-3 droplets and show that, not only do these droplets shrink at slower rates for higher salt concentrations, they also show that larger droplets shrink slower than smaller droplets.

Contents

1 Introduction **7**

2 Theory **11**
2.1 Ostwald ripening 11
2.2 Confocal laser scanning microscope 11

3 Methods and materials **15**
3.1 Types of samples 15
3.2 Microscope 18
3.3 Measurements 19
3.4 Image processing and analysis 21
3.4.1 ImageJ 21
3.4.2 Python 21

4 Measurements, results and analysis **25**
4.1 Reference measurement 26
4.2 Control: Imaging 27
4.3 Longer timescale 29
4.4 Control: Evaporation 31
4.5 Control: Drift 33
4.6 Multi Well Plates 34
4.6.1 P5K25 34
4.6.2 P10K100 36
4.6.3 P15K100 37
4.7 PLL-g-PEG coating 40
4.8 General 42

5 Discussion **45**
5.1 Reference measurement 45
5.2 Control: Imaging 46
5.3 Longer timescale 47
5.4 Control: Evaporation 48
5.5 Control: Drift 48
5.6 Multi Well Plates 48
5.7 PLL-g-PEG coating 51
5.8 General 53

6 Conclusion and outlook **55**

7 Appendix **59**
7.1 Code 59
7.2 Data parameters 66
7.3 Protocols 66

Chapter 1

Introduction

The field of cell biology has made incredible advancements during the last decades when it comes to understanding the many complex and interwoven processes that happen inside cells and how they are regulated. One of these advancements is the discovery of the existence of membraneless compartments inside cells, called biomolecular condensates or simply condensates [1].

Our current understanding is that these condensates are essential for quick responses, process inhibition and cell protection among many other functions. Cell compartments with membranes would be too slow or simply unable to control these processes, thus showing the importance of the condensates. Some processes where biomolecular condensates are involved are RNA metabolism, ribosome biogenesis or signal transduction, to name a few [1, 2]. Condensates are often comprised of proteins and nucleic acids. Figure 1.1 shows a number of condensates that exist in different types of eukaryotic cells.

These condensates not working like they are supposed to, can have large scale consequences. Research has found links between certain condensate behaviours and neurodegenerative diseases [3–5]. An example of this is the FUS protein, a condensate that, under certain conditions, irreversibly grows fibres. This fibre growth has been linked with the development Alzheimer's disease [5]. Understanding why and how these condensates are involved with neurodegenerative diseases could help identify causes and possibly find treatments or cures.

In vitro observations have shown that condensates exhibit liquid-like behaviour [6]. This liquid-like behaviour means that, like liquids, condensates can form droplets made up a dense congregate of proteins, held together by something that acts similar to the surface tension of fluids,

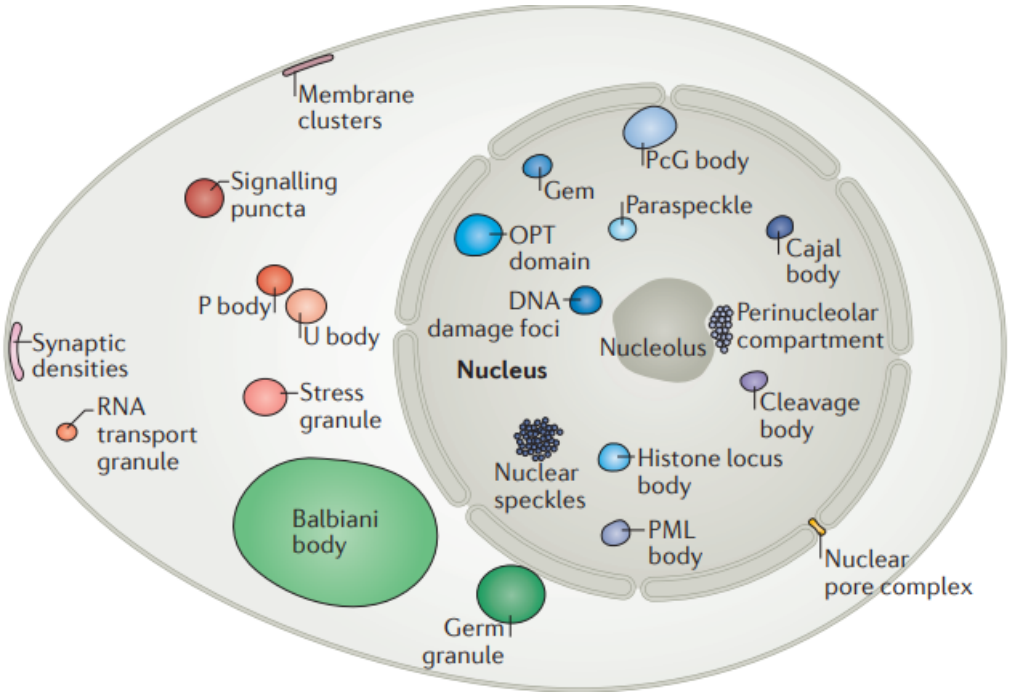

Figure 1.1: *Biomolecular condensates in eukaryotic cells. Not all condensates are present in all cells, here they are shown for completeness. Image taken from Biomolecular condensates: organizers of cellular biochemistry, Banani et al. 2017.*

and that these droplets can merge with each other. In other words, these condensates show properties of liquids. This liquid-like behaviour allows the condensates to undergo liquid-liquid phase separation. Studies have shown that liquid-liquid phase separation plays an important part in the organisation and formation of these condensates [7, 8].

Liquid-liquid phase separation is a form of phase transition where a homogenous solution spontaneously separates into two distinct immiscible liquids. A dense and a dilute phase. For this to happen, part of the liquid components needs to interact with itself more than with the rest of the components. In other words, it becomes a better solvent for itself than the solution it was initially dissolved in. This component becomes more concentrated in the dense phase [8]. Liquid-liquid phase separation can be visualised using a phase diagram, much like phase diagrams for other fluids, like water. Figure 1.2 shows a phase diagram of liquid-liquid phase separation. The black line separates the one-phase and two-phase regimes and is dependent on environmental conditions, for example the temperature or pH. Below the saturation concentration (c_{sat}), the solution is in the (dilute) one-phase regime. By increasing the concentration, the solution

enters the two-phase regime and demixes, a dense phase appears. Continuing to increase the concentration, along the tie line in the figure, leads to a point where the dense phase is the dominant phase. Eventually the whole solution has become the dense phase and only one phase remains. If the environmental conditions are above the critical point, no liquid-liquid phase separation occurs and the concentration rises uniformly.

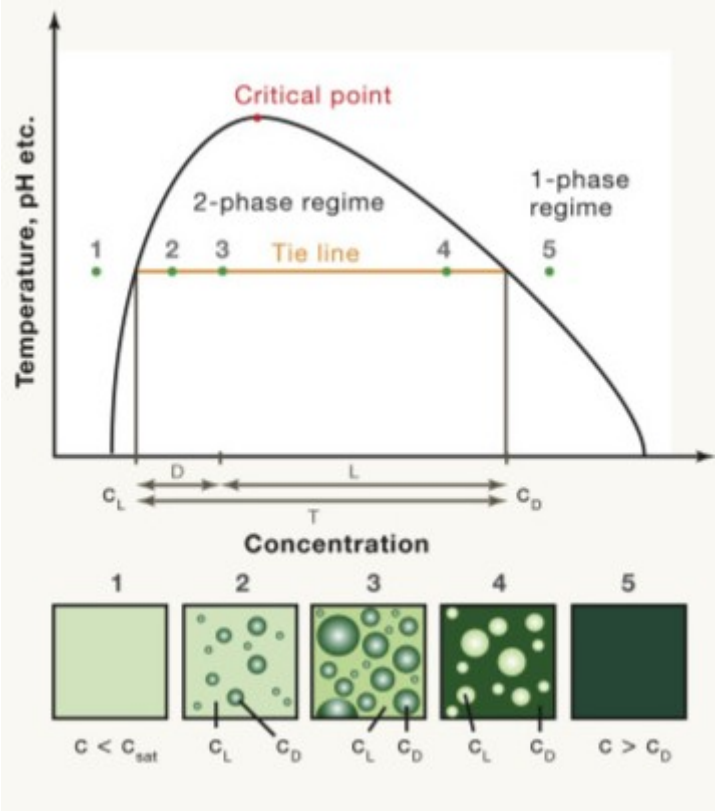

Figure 1.2: *A phase diagram of a liquid that experiences liquid-liquid phase separation. By increasing the concentration along a horizontal line (see the tie line) a liquid undergoes spontaneous demixing. The numbers in the graph belong to the numbered images below the graph, these images show what the liquid would look like at different points in the phase diagram. Image taken from Considerations and Challenges in Studying Liquid-Liquid Phase Separation and Biomolecular Condensates, Alberti et al. 2019.*

Understanding the liquid-like behaviour of the biomolecular condensates is of interest because it would help explain how processes in cells are regulated and may lead to other insights and developments in cell biology, like the link between liquid-liquid phase separation and neurodegenerative diseases mentioned earlier.

Some of these condensates, such as P-granules, show liquid-like be-

haviour [6]. P-granules are made up of multiple components, some of which can be proteins. PGL-3 is such a protein which also exhibits liquid-liquid phase separation behaviour.

Exclusively PGL-3 is studied in this research. Previous research has shown that the material properties of PGL-3 droplets differ depending on surrounding circumstances, an example of this is an increase in elastic modulus, viscosity, and surface tension as the salt concentration of the surrounding fluid decreases [9]. It has also been shown that these droplets experience something called glass-like ageing [10–12].

Glass-like ageing is a process where the material properties of a material change over time, similar to how glasses age. In the case of PGL-3, the ageing shows an increasing viscosity with age [12]. Through what mechanism the condensates age is not completely understood and is a current area of research [10, 11].

PGL-3 droplets also show another remarkable behaviour, they shrink over time [9, 13]. The result of Jawerth et al. 2020 is from looking at a single PGL-3 droplet in a $300mM$ KCl solution, this result roughly shows a 10% decrease in radius over the course of 1000 minutes. McCall et al. 2025 looked at multiple droplets in a $75mM$ KCl solution and found that the droplets shrunk 40 to 60 percent after 15 hours. Another thing they note is that it appears that initial shrink rate decreases with increasing initial radius.

It remains unknown why the droplets shrink. A reasonable consideration is that the shrinking behaviour could be related to the ageing of the droplets and their changing material properties. Do the droplets shrink at different rates when surrounded by different salt concentrations? Does this behaviour align with the earlier results?

In this research a suspected relation between the shrinking of PGL-3 droplets and the glass-like ageing is investigated. This is done by tracking the radii of the PGL-3 droplets over time using different salt solutions.

Chapter 2

Theory

2.1 Ostwald ripening

One process that will be looked at it Ostwald ripening. An estimate will be made to see if a larger initial radius leading to a lower initial shrink rate can be explained by this process.

Ostwald ripening is a phenomenon that occurs in colloid solutions with small insoluble particles dispersed inside a liquid medium. Over time the smaller particles dissolve and redeposit onto the larger particles. This could go on until there is one large particle left that contains all the matter. The average radius of the particles will increase over time as a result. A formula (equation 2.1) has been derived that gives the average particle radius over time [14]. This can give an estimate on the effect of Ostwald ripening on the PGL-3 droplets.

$$\langle R \rangle^3 - \langle R_0 \rangle^3 = \frac{8\gamma c_\infty v^2 D}{9 R_g T} t \tag{2.1}$$

The equation shows the relationship between the average radius R, average initial radius R_0 and time t. It is also dependent on a number of material properties. These are the surface tension of the particle γ, its solubility c_∞, its molar volume v and its diffusion coefficient D. On top of that it is dependent on the temperature. R_g is the ideal gas constant.

2.2 Confocal laser scanning microscope

To perform measurements and observe the PGL-3 droplets a microscope is needed. For this research a confocal laser scanning microscope (CLSM)

is used. This technique has some advantages and disadvantages over conventional (wide-field) fluorescence microscopes.

A conventional fluorescence microscope beams light on the whole fluorescent sample which in turn makes the whole sample emit light, which is detected by a photodetector. This method gives a lot of noise in the form of unfocussed background light, which gives blurring and less contrast in the image. A confocal microscope overcomes this through point illumination and a pinhole in front of the detector, this pinhole ensures that only light from the focus plane can be detected and thus filters out light that is out of focus, see figure 2.1. Because of this, the optical resolution is much better.

The downside of using a confocal microscope is that the signal intensity from the detector is much lower because much of the light is blocked by the pinhole. This means longer exposures times, or higher light source intensities, are often needed. This can be overcome by using more sensitive photodetectors or an amplification device.

Another downside of confocal microscopes is that the technique only scans a point of the sample at a time, so to scan the whole sample (in 2D or 3D) will take longer as the microscope will have to move horizontally across the sample for a 2D image and vertically on top of that, for a 3D image.

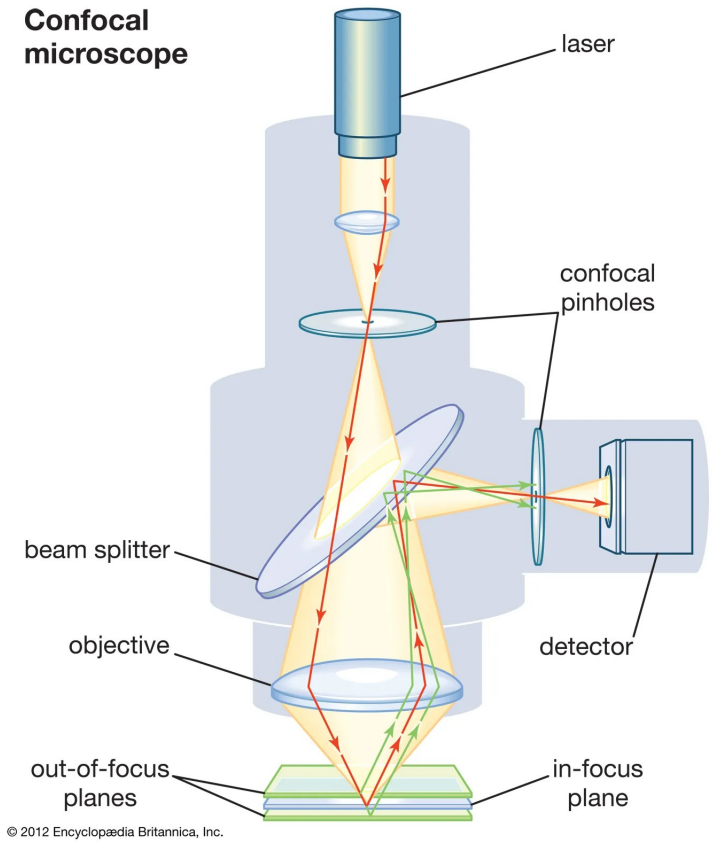

Figure 2.1: *Schematic of the working principle of a confocal laser scanning microscope. The laser emits monochromatic light which is focussed through a lens and a pinhole. It travels unhindered through a beam splitter and is focussed again by the objective onto the sample. Here the light excites the fluorescent sample and the emitted light travels back to the beam splitter, where it is reflected to a second pinhole. The light emitted from the focus plane of the sample is aligned so that it passes through the pinhole and is detected (red beam). The light emitted from out-of-focus planes is blocked by the pinhole (green beams). Credits: Encyclopaedia Britannica, Inc.*

Chapter 3

Methods and materials

The method of gathering and analysing PGL-3 data consists of the following steps. The samples are made by mixing PGL-3 protein with other substances according to section 3.1. The samples are placed in a confocal laser scanning microscope (see section 2.2 and 3.2), where they are observed. The collected data, recorded in the form of a video in nd2 format following section 3.3, is loaded into ImageJ, a special image processing software. ImageJ processes protein droplets in the video to make their largest radius appear in the same focal plane via the method described in 3.4.1. In python the droplets are identified and tracked by code described in 3.4.2, which also calculates and tracks the radius of the droplets over time. There the average ratio of radius over initial radius is found and from there the shrinking behaviour of the PGL-3 droplets can be quantified.

3.1 Types of samples

The sample solution is made by diluting protein stock to the desired PGL-3 and KCl concentrations such that liquid-liquid phase separation occurs. The PGL-3 is made locally in the lab by someone else from the group following the protocol of figure 7.1, the specific protein is PGL3-TEV-His6-EGFP. This solution consists of milliQ ultrapure water, KCl and the PGL-3 protein. A 7.3 pH buffer is also present (HEPES) as well as a reducing agent (DTT) for stability of the solution, with a concentration of $25mM$ and $1mM$ respectively. These substances are mixed to get a sample with the desired salt and protein concentrations. The ageing of the PGL-3 begins as soon as the sample solution is mixed, the wait time (τ_w) is the time between the mixing of the sample and the start of the measurement.

Since there are multiple different sample solutions a naming convention is used for this thesis. This naming convention states the first letter of the protein that is used with a number after it, signifying its molarity in μM. Then the metal from the salt is mentioned, since chlorine is always used, with a number signifying its molarity in mM. An example would be P15K100, this sample solution has 15 μM PGL-3 and 100 mM KCl.

The sample is made of two glass slides (epredia cover slips, 24x60 mm #1,5 or 22x22 mm #1,5) which are coated with a layer of PEG-silane. The coating is used to prevent wetting of the droplets on the glass slides, and is applied following the protocol of figure 7.2. A piece of double sided adhesive tape, called a spacer, is placed between the glass slides. The tape has a hole in the centre, this hole is the well in which the sample solution is pipetted, between $2 - 3\mu l$. It is important that the tip of the pipette does not touch the slide and that the sample solution does not fall and splash but is gently placed upon the slide. This is to not damage the coating on the slide and for safety when working with biochemical substances.

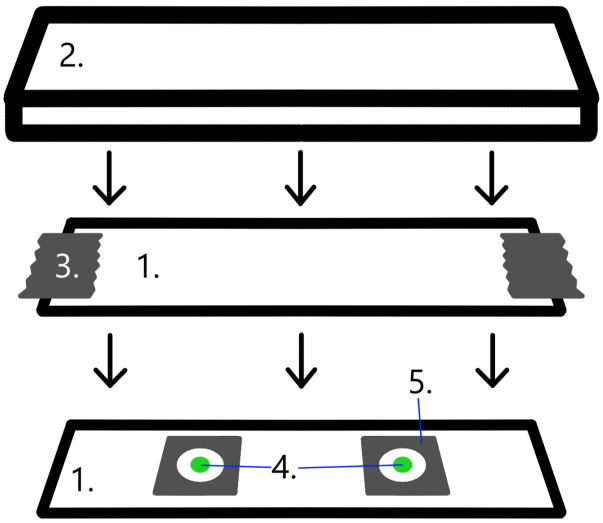

Figure 3.1: *Schematic of a glass slide sample with labelled components. 1) Glass slide with PEG-silane coating. 2) Microscope glass slide. 3) Double sided adhesive tape. 4) The sample solution placed in the wells, away from the edges of the well. 5) The spacer, double sided adhesive tape with a hole in the centre.*

A schematic of a made sample with labels of components is given in

figure 3.1. The spacer (5) is placed on one of the glass slides (1). Pipette the sample solution (4) into the well. Covering the well with the other glass slide seals it. To be able to place the sample in the microscope a microscope glass slide (2) is used, the sample is taped to this microscope glass using double sided adhesive tape (3).

Figure 3.2 shows an actual sample where some of the components are outlined and numbered with the same labels as in the schematic. The red square outlines (3) are the double sided tape, the round red outlines are the sample solution (4) placed inside the wells (the green circular outlines). The smaller square outlines are the outer edge of the spacers (5). In this sample two smaller square coated glass slides were used as the middle glass slide, which can be seen as the larger square green outlines.

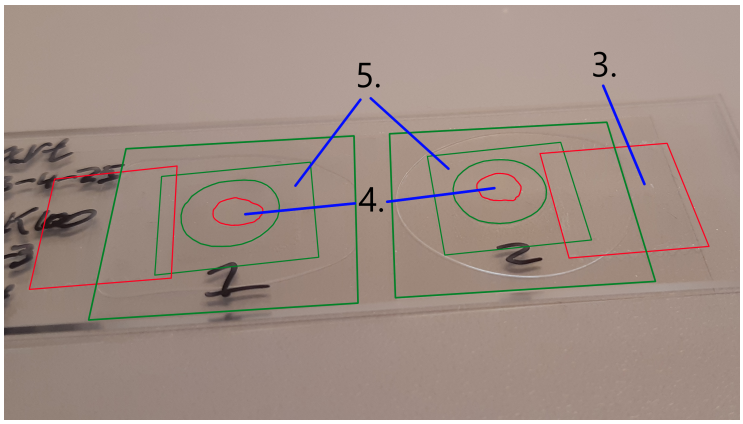

Figure 3.2: *A sample of P15K100. with the wells labelled as 1 and 2. The same labels from the schematic are shown with lines towards their corresponding areas. The red squares are the double sided tape. The round red areas are the sample solutions inside the wells. The area between the smaller green squares and green circles are the spacers. The larger green squares are two 22x22 mm glass slides that seal the wells individually.*

A different way of preparing samples is by using a multi well plate seen in figure 3.3, this is a plate with a grid of wells in which sample solutions can be placed. These wells are sealed with a sticker and a lid.

The multi well plate has the benefit of being able to do multiple measurements. The glass slide samples have one or two wells, so at most two measurements can be performed at a time, whereas using a multi well plate one can use as many as the other aspects of the measurement settings allow. Despite the area of the wells being smaller than with the glass slide samples, more sample solution is needed per well, around $10 - 20\mu l$. To ensure there is no evaporation, the sample solution is covered with silicone oil. As the oil is less dense, it sits on top of the sample sealing the

well.

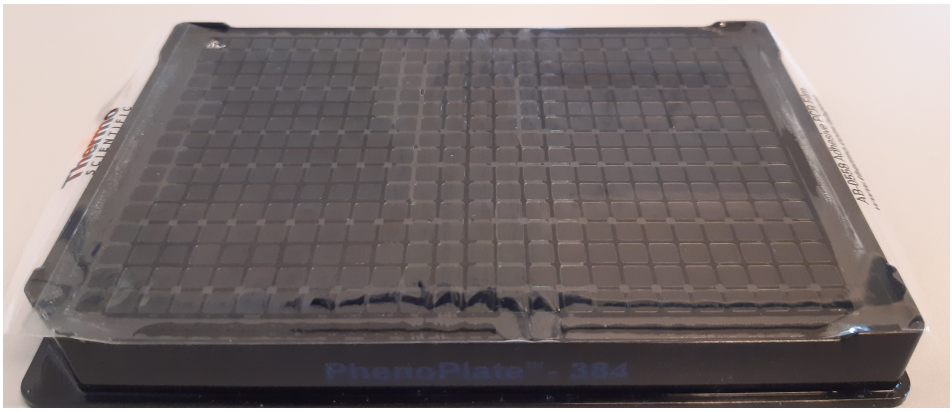

Figure 3.3: *A multi well plate with cover sticker and without lid.*

The last way to make samples is very similar to the method of preparing glass slide samples, as most of the steps are identical. The difference is that the glass slide on the bottom uses a different coating. Instead of the PEG-silane coating, the slide is coated with poly(L-lysine)-graft-poly(ethylene glycol) co-polymer or PLL-g-PEG (SuSoS, DÃŒbendorf). The PLL-g-PEG coating locks the droplets in place, which makes tracking the droplets easier and prevents data loss from droplets moving out of frame during measurements. With the PLL-g-PEG coating, the droplets wet slightly more than with the PEG-silane coating but not enough to be of concern, the droplets in figure 3.6 are still mostly spherical.

The plasma cleaner that was used to prepare the PLL-g-PEG coated slides was a Harrick Plasma PDC-002-CE, it was used following its manual.

3.2 Microscope

The microscope used in this research was a Nikon ECLIPSE Ti2 equipped with a VisiTech VT-iSIM system between the microscope and photodetector. This system uses confocal structured illumination microscopy (CSIM), a super-resolution imaging technique, and also essentially allows for many pinholes to be run in parallel, instead of the one pinhole of a regular CLSM. In figure 3.4 the microscope setup is visible. On the right side of the table stands the microscope. The black and blue box connected to the left side of the microscope is the VisiTech system. The photodetector is mounted on

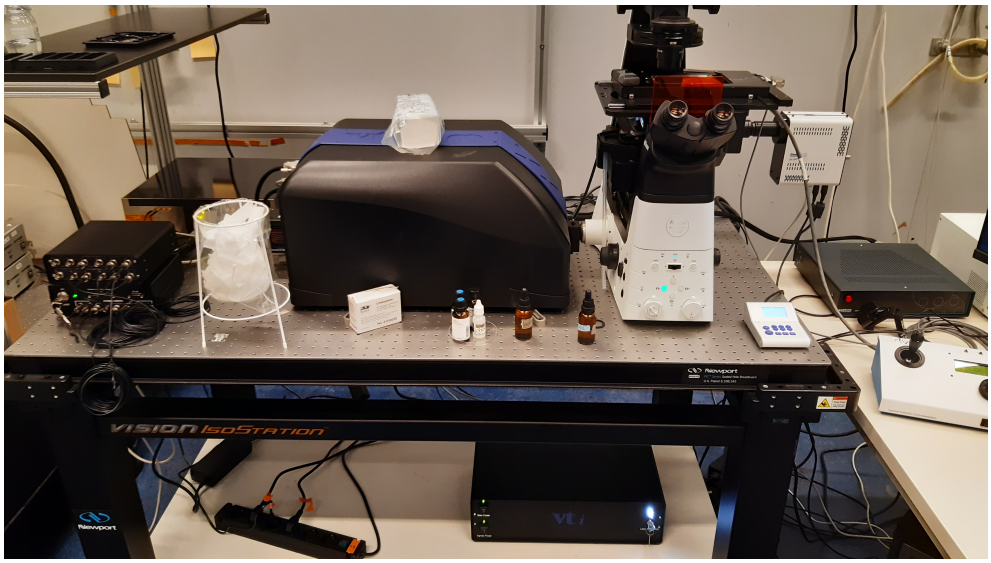

Figure 3.4: *Complete microscope setup. The Nikon microscope stands on the right side of the table. Connected to it is the VisiTech scanning system, the black box with blue stripe. The photodetector is connected to the left side of the scanning system. The power supplies are on the left or below the table.*

the left side of the VisiTech system, it is a 1T-01-PRIME-BSI-EXP detector from Teledyne Photometrics.

The other components, inside the microscope, that are relevant to this setup are the laser ($488nm$), the stage that is used to move the samples around (Applied Scientific Instrumentations, Inc., Product: MS-2000-500, Model: WK-XYB-APZ30-TI2000FT) and the objectives (Nikon Plan Apo λD 20x/0.80 and Nikon Plan Apo λ 40x/0.95, correction collar should be at 0.17).

The microscope can be operated with a computer using software specific to the microscope. All measurement settings can be chosen using this software.

3.3 Measurements

The samples are placed inside the platform seen in figure 3.5. Using the software belonging to the microscope measurements are taken. The recorded data is a video file in nd2 format.

Some considerations regarding the nature of the sample solutions are made in the measurement settings. The protein droplets in the sample solution can move, so the frame rate should be high enough to be able to

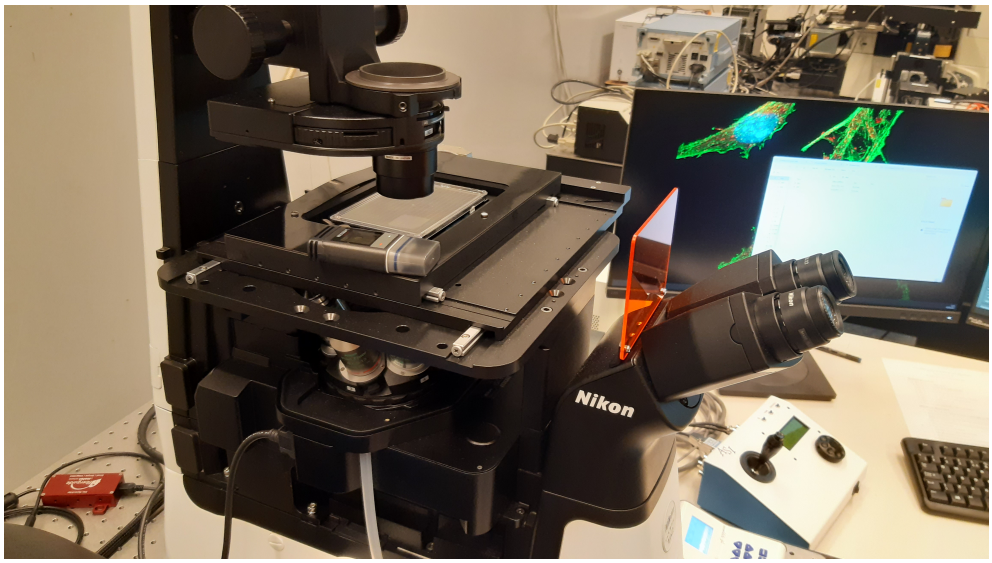

Figure 3.5: *The microscope up close. The movable stage in the centre holds a platform in which the samples are placed, here with a multi well plate inside the platform. The laser hovers above the sample and points downwards. Below the stage are the objectives.*

track the droplets. The total measurement time should be long enough to track the shrinking behaviour of the droplets. The chosen light source needs to have the right wavelength to make use of the fluorescent properties of the protein (see previous section). The droplets are not the same size, so to accurately track the radii, images need to be taken at multiple heights or focal planes.

This last consideration needs further elaboration. To accurately find the radius of a droplet when looking from above, an image needs to be taken at the height where the droplet appears biggest. But because the height where this is the case depends on the radius, it is needed to take images at different heights. To solve this, a z-stack is made for each frame in the video, this means that every frame is a stack of images or slices. To ensure that all droplets are correctly accounted for, the boundaries of the z-stack are set so that the first and last slice are above and below the droplets. Figure 3.6 shows a vertical slice of one of the samples, so a side view of a z-stack. The different sizes of droplets are clearly visible, with the the largest radius of the droplets being at different heights. See the left- and rightmost droplets for example, the leftmost has its largest radius below the horizontal yellow line while the rightmost has its largest radius above the line.

All the measurement settings are stored in a metadata file that is produced with each taken measurement. This file can be accessed by opening

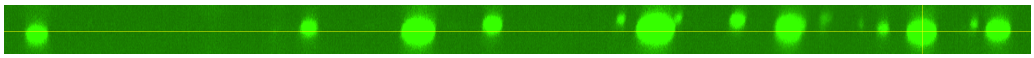

Figure 3.6: *A side view of the z-stack of one of the samples. This vertical slice shows droplets of different sizes at different heights. Along the horizontal yellow line is what would be visible when looking at a singular image.*

the nd2 video file with ImageJ. Some of these settings are shown in the table with data parameters in the appendix.

3.4 Image processing and analysis

The raw data is processed and analysed in two parts. First a maximum intensity projection is made using ImageJ, then the droplets are identified and tracked in python. After filtering the resulting data, the radius over time is plotted.

3.4.1 ImageJ

ImageJ is a Java written, open-source image processing and analysis software. It is used to extract the metadata of each measurement, and to get a maximum intensity projection of the nd2 video file. This maximum intensity projection looks at a pixel of a single frame and compares intensity values of that pixel for each slice of the z-stack, then it takes the highest value. It does this for all pixels and all frames. This projection collapses the z-stack of a frame into one single slice where all droplets appear at their biggest in the same focal plane. This maximum intensity projection video file is saved as an image sequence, where the individual images are .TIF files, and is loaded into python.

3.4.2 Python

The image sequence is loaded into python where multiple steps are taken to find the radii over time. After applying a threshold, the contours of the droplets are found using the OpenCV package. A minimum enclosing circle is fitted to these contours, the centre and radius of the fitted circle are stored in a dataframe together with the frame number. For sufficiently small droplets, the uncertainty in their radius is too big so these droplets are discarded, this is done by setting a minimum radius for the droplets. This size limit is not fully investigated but a safe value is set, which can be found in the data parameters table in the appendix.

The identified droplets from the dataframe are linked using the trackpy package, which results in a new dataframe where all the droplets are given their own label. Trackpy links the droplets by selecting the best candidate of all droplets in the next frame. Using a maximum search range speeds up this process because it will only consider droplets within a circle with the radius of that search range, thus needing to consider less droplets. On top of that, using a maximum search range improves the accuracy of the linking process.

A useful way of visualising the radius over time data is by calculating, and plotting the ratio of radius over initial radius (r/r_0) over time, this way the data collapses roughly onto a single curve. An example of this can be seen in figure 4.5a and 4.5b.

Between calculating r/r_0 and plotting, filters need to be applied. Since droplets behave liquid-like and are able to merge, the radius of a droplet can jump between frames. They can also move in or out of frame, in which case the radius can also show a big jump between frames. Other droplets are only present for a short amount of time and don't show any shrinking in that timespan. To deal with this, two filters are applied. The first is a filter that discards droplets that are present in fewer frames than a set parameter. The other filters based on the maximum allowed change in the ratio r/r_0 between consecutive frames. Both of these parameters can be found in the sample parameters table.

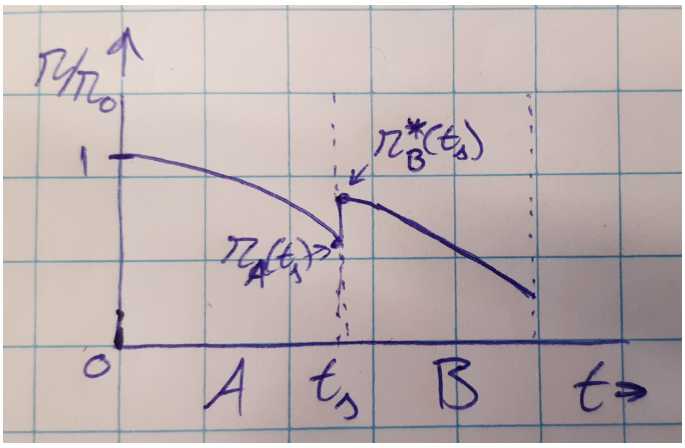

Figure 3.7: *A droplet jumps in radius at t_s. The code splits the droplet into part A and part B. Part A remains unchanged, part B is rescaled so that $r_B(t_s) = r_A(t_s)$ is true.*

The rate of change filter works like this, whenever the absolute value of the difference in ratio is larger than the maximum allowed change, the droplet data is split into two parts. Part A of the data remains belonging to

the same droplet. Part B is identified as a new droplet and gets a new label, the initial ratio of part B is set to be the same as the last ratio of part A. See figure 3.7 below for an example. If the data is split at t_s, the code ensures that $r_B(t_s) = r_A(t_s)$ by rescaling all of $r_B(t)$ through $r_B(t) = \frac{r_A(t_s)}{r_B^*(t_s)} r_B^*(t)$, where the * signifies the unscaled ratios of part B.

After applying the filters, the average ratio r/r_0 is found for every frame along with the standard deviations. This data is saved in its own file.

By plotting the averages of all measurements in one figure, the differences between samples and behaviour at different conditions can be shown more clearly.

Chapter 4

Measurements, results and analysis

This chapter will show the specifics, results, and analysis of the measurements taken with the general setup of chapter 3. Each section will treat a different measurement, relevant information will be mentioned in those sections and can also be found in the sample parameters table in the appendix (section 7.2).

For a first look, a reference measurement was taken (sections 4.1 and 5.1), to get a feel for the relevant parameters of measurements. Section 4.1 treats the results and analysis of this measurement while section 5.1 discusses the findings.

To see if taking a measurement, and exposing the sample to the laser in the microscope, had any effect on the protein droplets, a control measurement was taken (sections 4.2 and 5.2). In sections 4.3 and 5.3 a longer measurement time was used to see if shrinking occurs at longer measurement times.

Another control measurement was taken (sections 4.4 and 5.4) to check whether adding silicone oil around the spacer prevented evaporation. Sections 4.5 and 5.5 treat the drift of droplets present during the measurements. Multiple results, obtained using the multi well plate method, are shown in section 4.6 and discussed in section 5.6. The method using the PLL-g-PEG coating gave the results of section 4.7 and are discussed in section 5.7.

Lastly, all obtained results are compared and discussed as a whole in sections 4.8 and 5.8. The estimation of the Ostwald ripening is made. It also contains a table with an overview of the measurements, their purpose and the relevant figures.

4.1 Reference measurement

For the reference measurement a P15K100 ($15\mu M$ PGL-3, $100mM$ KCl) sample was used, prepared using the first method of section 2.1. 3 μl sample solution was used in each well. The microscope was set to make a z-stack every 5 minutes with a total measurement time of 23 hours, 40 minutes. This measurement was done to get a feel for the relevant parameters. The sample parameters for this measurement are listed under sample P15K100S1.

Following section 2.4 the raw data is processed. Figure 4.1 shows (a) the max intensity projection of the raw data,(b) the data after the threshold and (c) the found contours respectively.

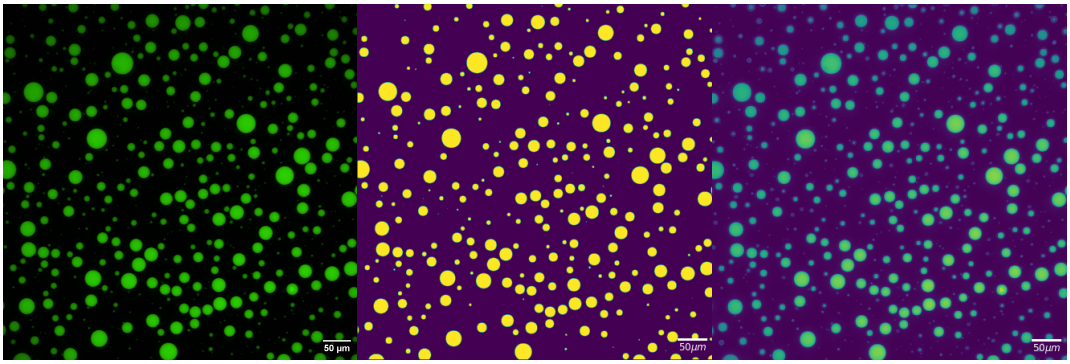

(a) ***(b)*** ***(c)***

Figure 4.1: *The first frame of the P15K100S1 sample. (a) The max intensity projection of the raw data. (b) The data after applying the threshold. (c) The contours found after the applying the threshold, the areas within the contours are coloured in.*

Performing the analysis, the filter parameters were set to a minimum radius of 5 pixels, a minimum presence of 25 frames and a maximum allowed rate of change of 1.5% for the ratio. This results in figures 4.2a and 4.2b. The black line in figure 4.2b is the average ratio of r/r_0 over time.

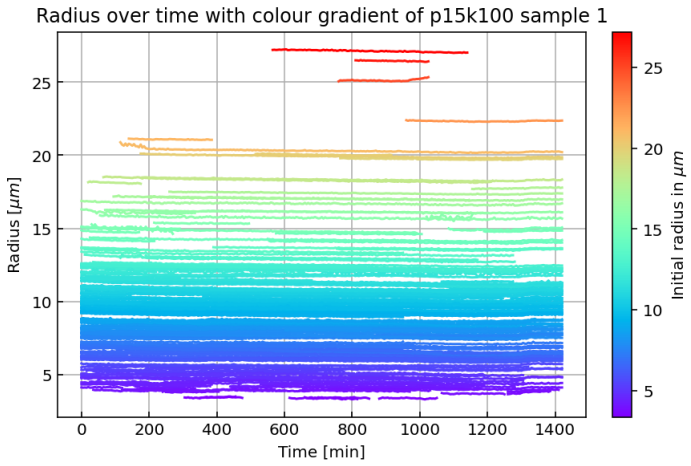

(a)

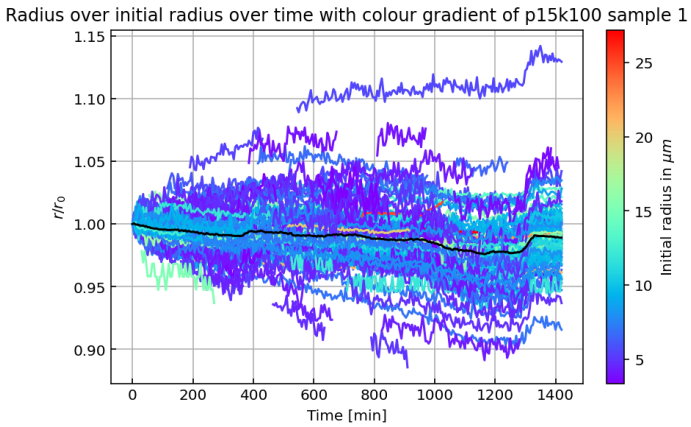

(b)

Figure 4.2: *Time plots of the P15K100S1 sample with colour gradient. (a) Radius in μm. (b) r/r_0 including the average ratio (black line).*

4.2 Control: Imaging

This measurement was done to see if exposure to the laser from the microscope had influence on the droplets and their shrinking behaviour. A P15K100 sample was used for this, prepared using the first method of section 2.1. 3 μl sample solution was used in each well. The microscope was set to make a z-stack every 10 seconds with a continuous measurement time, meaning it needed to be stopped manually. It took roughly six seconds complete a z-stack, making the exposure to the laser relatively continuous compared to other appropriate frame rates. Due to storage

space limitations this measurement was stopped after roughly 19 hours. The sample is listed as P15K100S2.

Following the analysis steps resulted in figures 4.3a and 4.3b, where the used parameters were a minimum radius of 5 pixels, a minimum presence of 120 frames and a maximum allowed rate of change of 1.5% for the ratio.

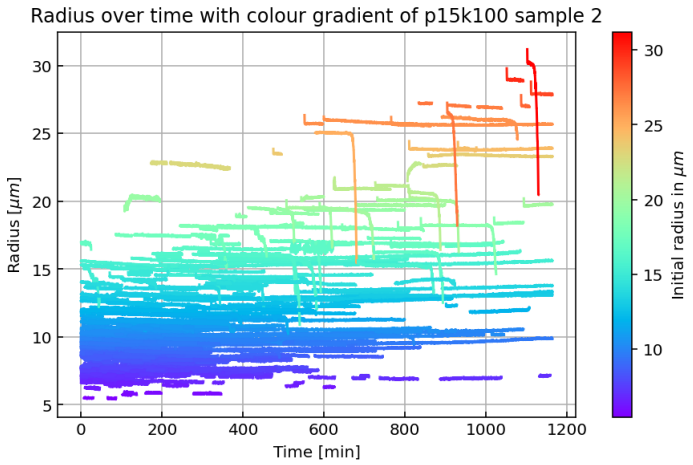

(a)

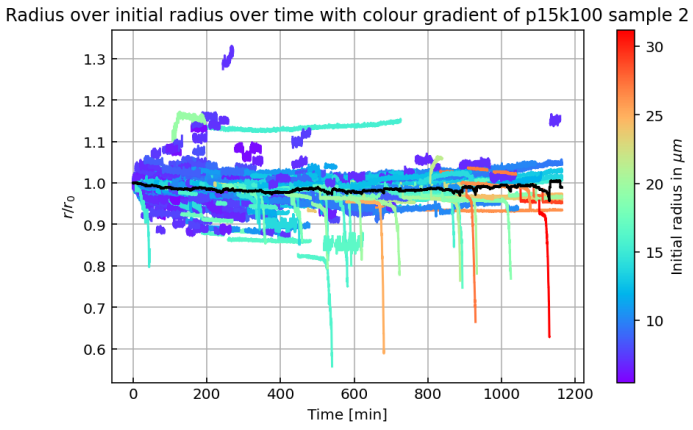

(b)

Figure 4.3: *Time plots of the P15K100S2 sample with colour gradient. (a) Radius in μm. (b) r/r_0 including the average ratio (black line).*

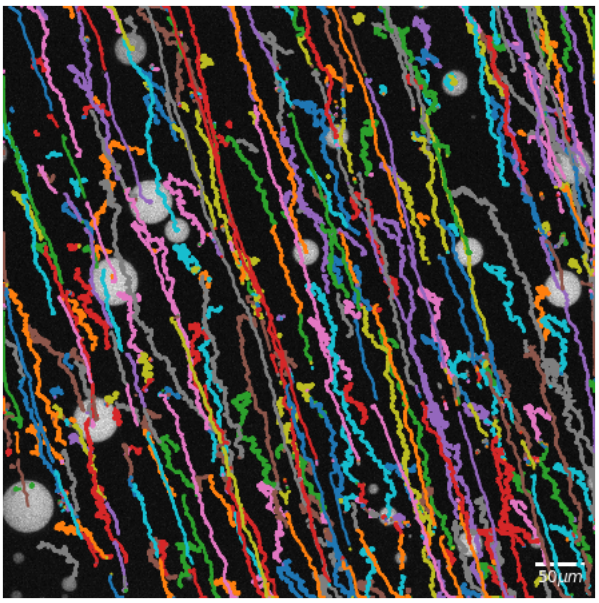

Figure 4.4: *The tracks found by trackpy shown on top of the last frame of the P15K100S2 sample.*

A noteworthy observation is that the droplets tend to move in a set direction. Figure 4.4 shows the drift of the droplets, downwards and to the right.

4.3 Longer timescale

For this measurement a longer measurement time was set to see if the shrinking of the droplets starts after a longer time than previously seen. A P15K100 sample was used for this, with 3 μl sample solution in each well. For this measurement silicone oil was added around the outside of the spacer to prevent evaporation of the water inside the sample solution. Enough oil was added to ensure the spacer was completely surrounded, this was roughly $20 - 30\mu l$ per well. The oil was added after the wells were sealed but before the microscope glass was put in place.

At a frame rate of one z-stack every 15 minutes for a total measurement time of 150 hours (6.25 days), performing the measurement and analysis steps resulted in figures 4.5a and 4.5b. The used parameters were a minimum radius of 5 pixels, a minimum presence of 25 frames and a maximum allowed rate of change of 3% for the ratio. This sample is listed as P15K100S3.

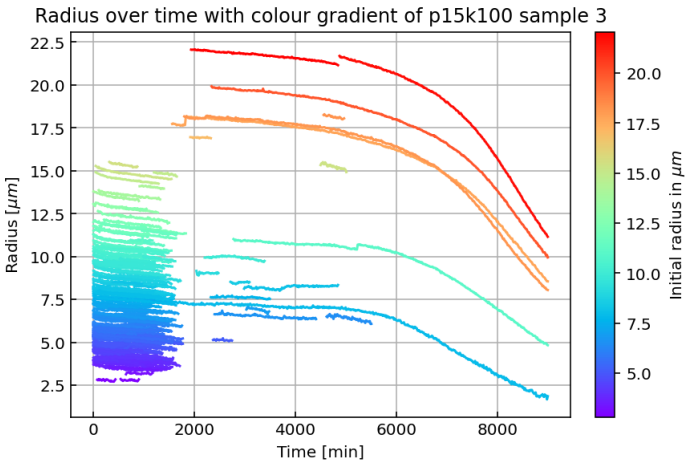

(a)

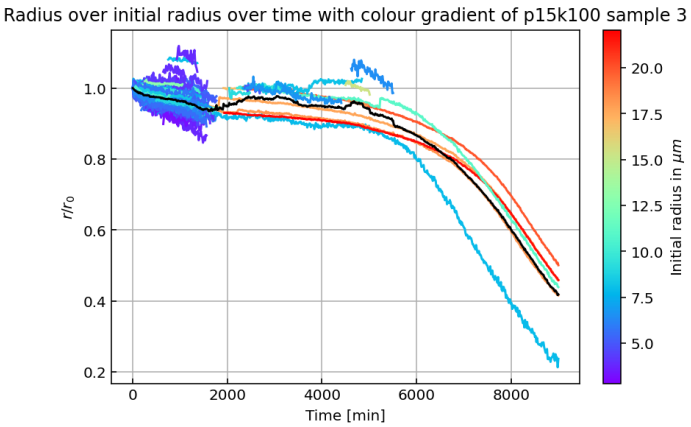

(b)

Figure 4.5: *Time plots of the P15K100S3 sample with colour gradient. (a) Radius in μm. (b) r/r_0 including the average ratio (black line).*

The drift referring to figure 4.4 also shows up in this measurement, as can be seen in figure 4.6.

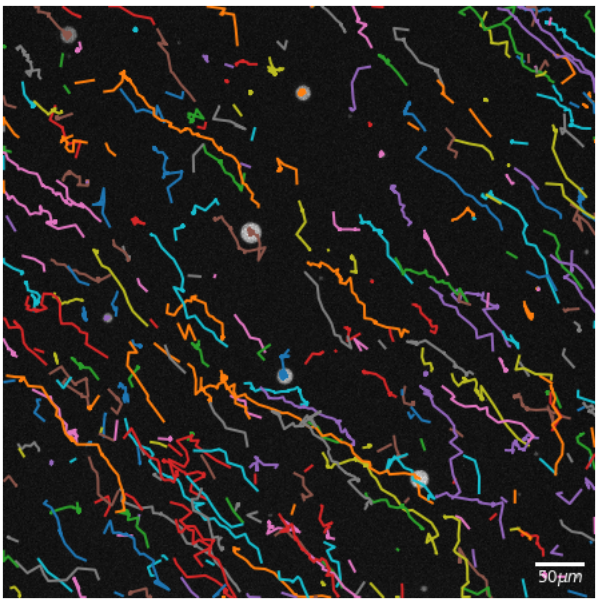

Figure 4.6: *The tracks found by trackpy shown on top of the last frame of the P15K100S3 sample.*

4.4 Control: Evaporation

The purpose of this measurement was twofold. By letting the sample sit for a day before starting the measurement, the droplets should have settled completely and move around much less. Thus giving answer to one of the possibilities for the drift. The sample would sit in the same environment as it would during the measurement. Since the droplets of P15K100 samples don't appear to notably shrink in the first two days, no noteworthy amount of information would be lost by waiting. The other purpose was to see how the silicone oil around the spacer influences evaporation, as this was not clear from the previous measurement. This was done by looking at the whole sample before and after the measurement and the recorded data.

Another P15K100 sample was used, with $3\mu l$ sample solution in each well with silicone oil added around the outside of the spacer. With a frame rate of one z-stack every 12 minutes for a total measurement time of 120 hours, the following results were found. Figure 4.7 shows the raw data in the first and last frame. Figure 4.8 shows the sample before and after the measurement. Lastly, figure 4.9 shows the tracks found by trackpy.

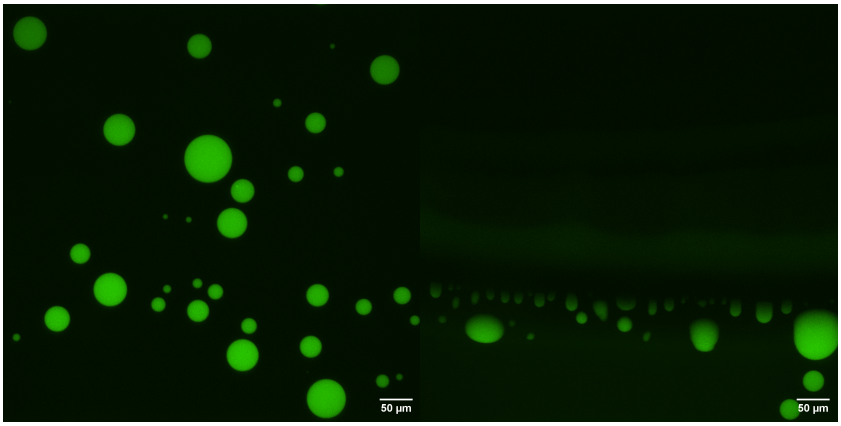

(a) *(b)*

Figure 4.7: *The max intensity projection of the raw data of the P15K100 sample. (a) The first frame of the sample. (b) The last frame of the sample. The faint horizontal green line is the edge of the sample solution, above that line no solution is present.*

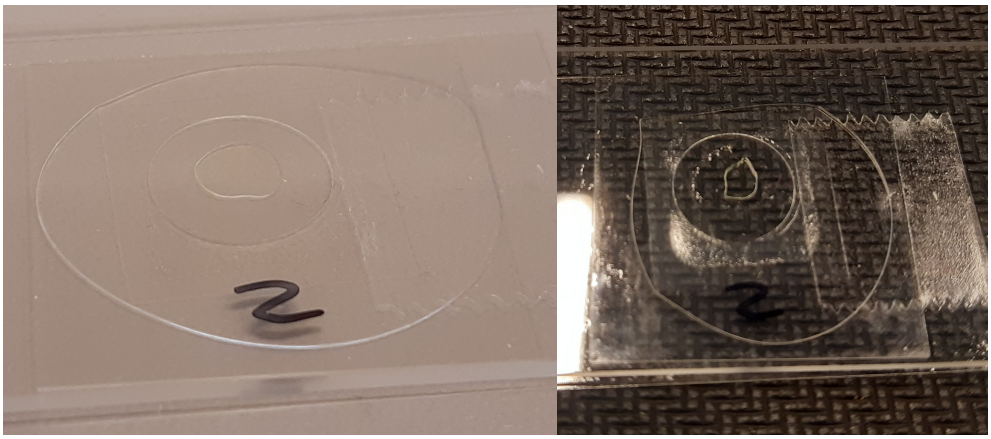

(a) *(b)*

Figure 4.8: *The used sample well with solution and silicone oil. (a) The well before the measurement, the silicone oil has completely surrounded the spacer. (b) The well five days after the before photo was taken. Over half of the solution evaporated. Some of the silicone oil got between the spacer and glass slides, the more opaque sections, mostly around the bottom and right sides of the well, is where the silicone oil got inside.*

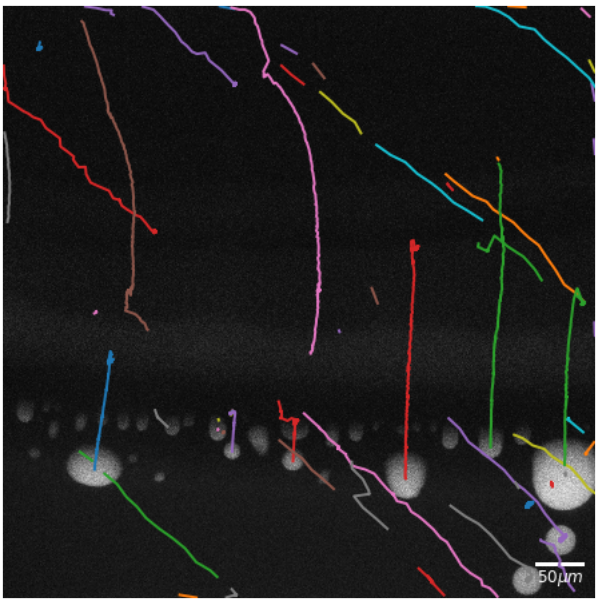

Figure 4.9: *The tracks found by trackpy shown on top of the last frame of the P15K100 sample from the evaporation control measurement.*

4.5 Control: Drift

The next measurement was meant to prove that the issue of drift had to do with something not being level, as that was the suspected cause. At the same time, a different type of sample was used, a multi well plate (see figure 3.3). The use of a multi well plate in this case was mostly to learn how to use this type of sample for future measurements, because of the benefits described in section 3.3.

This measurement was done in two parts. With a P15K100 sample solution of 18μl with 40μl of silicone oil on top, two short measurements were taken with part A having 12 minutes between z-stacks for a total time of 12 hours and part B having 15 minutes between z-stacks and a total time of 135 minutes. Both used the same sample, where for part B, the sample was turned around. This meant that the lower right corner of the well in part A became the upper left corner of the well in part B. The tracks found by trackpy are shown in figure 4.10. In both cases the droplets moved towards the lower right corner. The tracks that move straight down on the right side of figure 4.10a are moving along the wall of the well.

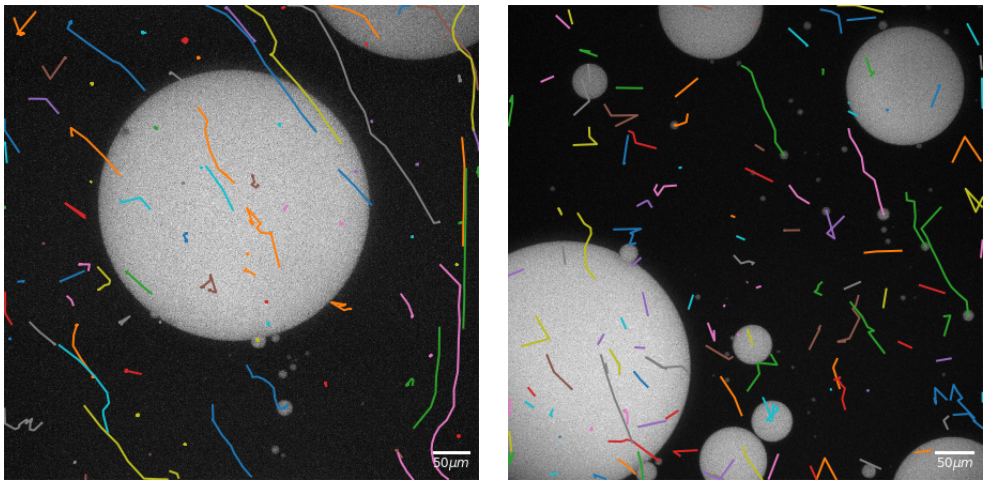

(a) *(b)*

Figure 4.10: *The tracks found by trackpy plotted on top of the last frame of the drift control measurements. (a) Part A. (b) Part B.*

4.6 Multi Well Plates

After the microscope table was level again, multiple measurements were taken using the multi well plate with different solutions to gather data about different conditions for shrinking. The used solutions were P5K25 and P10K100 as well as more P15K100 samples. Again, P15K100 means a sample solution with $15\mu M$ PGL-3 and $100mM$ KCl. The results are shown grouped by sample solution.

4.6.1 P5K25

The first P5K25 measurement was done with $18\mu l$ sample solution and a measurement time of 72 hours with 6 minutes between z-stacks. This sample is listed as P5K25S1, where the other analysis parameters can be found. Due to the small droplet sizes compared to previous samples, a 40x objective was used instead of the 20x objective. This resulted in an issue in the analysis. There was background noise interfering with the code that identifies the droplets, making the code unable to produce results. Figure 4.11 shows how the background noise interfered with the identification of droplets, the light from the laser created a ring of oversaturation during the measurement. However, this oversaturation only became an issue for the program after 165 frames, so by selecting the first 165 frames and per-

forming the analysis on those the results of 4.12a were found. Another thing to note is how the droplets barely moved during this measurement, as can be seen in 4.12b.

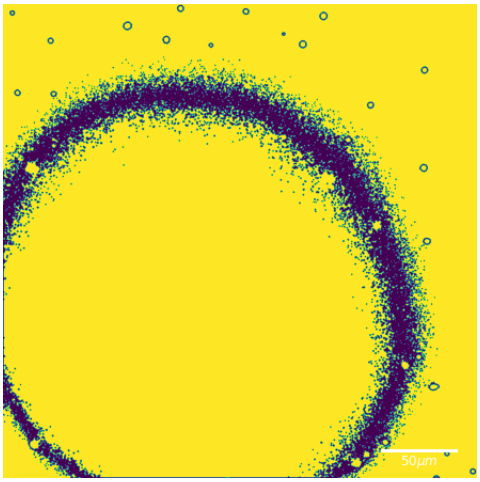

Figure 4.11: *The data found in the last frame of the P5K25S1 sample after applying the threshold with the ring of oversaturation is clearly visible.*

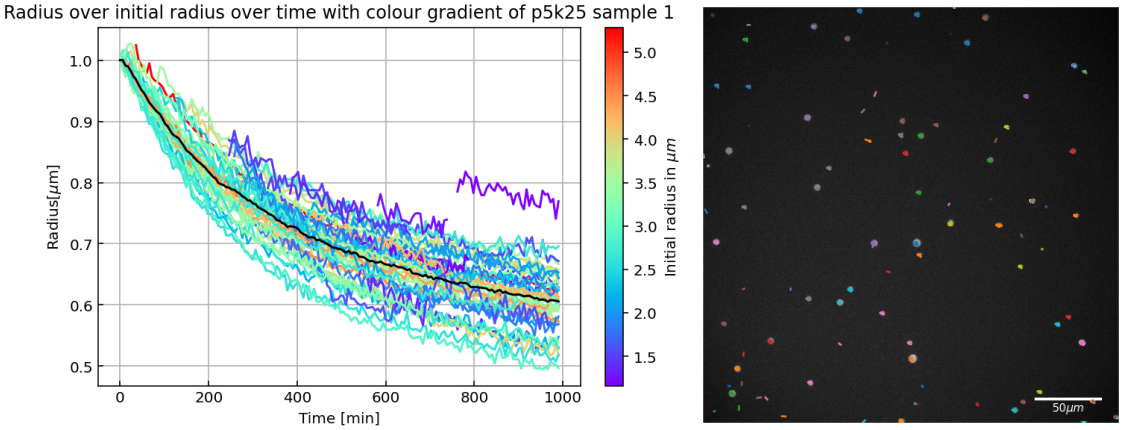

(a) ***(b)***

Figure 4.12: *P5K25S1 data. (a) The r/r_0 over time with a colour gradient to indicate the initial radius. Only data from the first 165 frames is shown. (b) The tracks found by trackpy shown on top of frame 165.*

For the second measurement, a measurement time of 44 hours was used with a z-stack every 5 minutes. This time the droplets were large

enough to use the 20x objective again. $20\mu l$ of P5K25 solution was added to the well, with $40\mu l$ of silicone oil to cover it. The used analysis parameters are listed under P5K25S2. The results of the measurement are shown in 4.13.

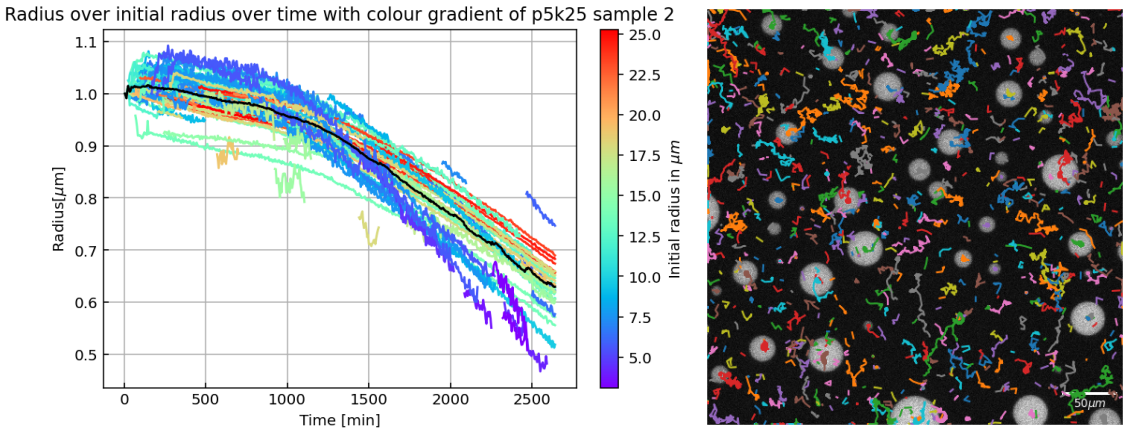

(a) ***(b)***

Figure 4.13: *P5K25S2 data. (a) The r/r_0 over time with a colour gradient to indicate the initial radius. (b) The tracks found by trackpy shown on top of the last frame.*

4.6.2 P10K100

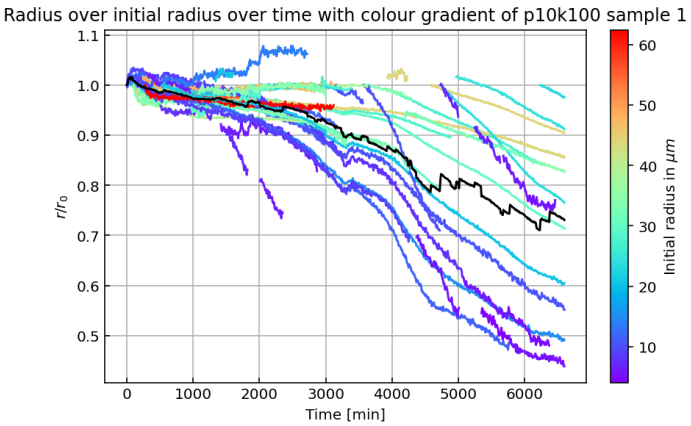

Figure 4.14: *r/r_0 over time of the P10K100S1 sample with a colour gradient to indicate the initial radius.*

The first P10K100 measurement used 18μl sample solution and 40μl of silicone oil. A z-stack was taken every 10 minutes for a total duration of 110 hours. The analysis parameters can be found under P10K100S1. The results of the analysis are shown in figure 4.14.

For the second P10K100 measurement three wells were measured at the same time using the same sample. Each well had 15μl and 30μl of sample solution and silicone oil respectively. A z-stack was taken every 10 minutes for a total time of 94 hours. The analysis parameters are the same for each well and can be found under P10K100S2. The results of each well are shown in figure 4.15 on the next page. Note that the time axes for each are different. This is because in well one and two, no more droplets were present in the field of view after a certain time. For trackpy to work, at least one droplet needs to be present in every frame, so to make sure the code worked all empty frames were discarded, resulting in different times for the final frames with droplets still present.

4.6.3 P15K100

Another multi well measurement was done with three wells at the same time using a P15K100 solution. Each well had 15μl of sample solution and 30μl of silicone oil on top. The measurement ran for 120 (5 days) hours with a z-stack every 12 minutes. The analysis parameters can be found under P15K100S7, again all three wells used the same parameters in the analysis. The results thereof are shown in figure 4.16 two pages over.

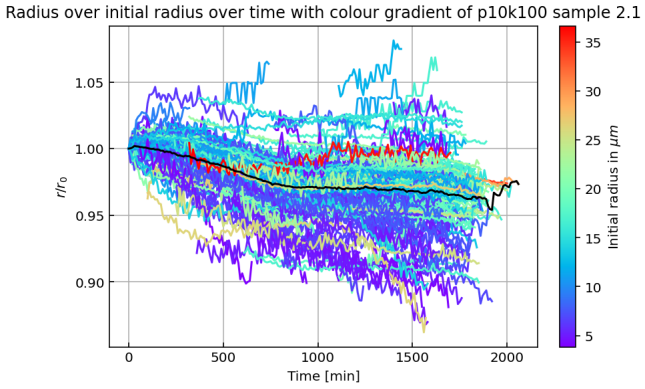

(a)

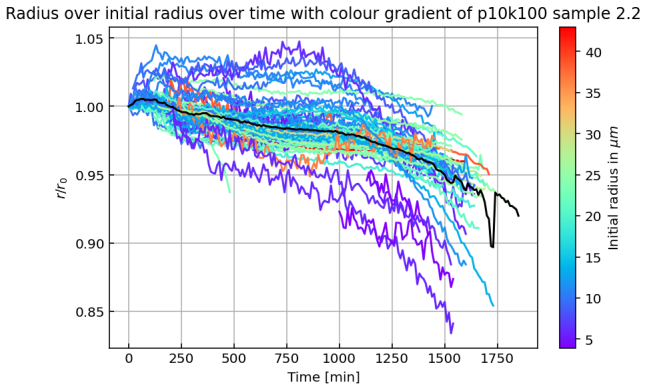

(b)

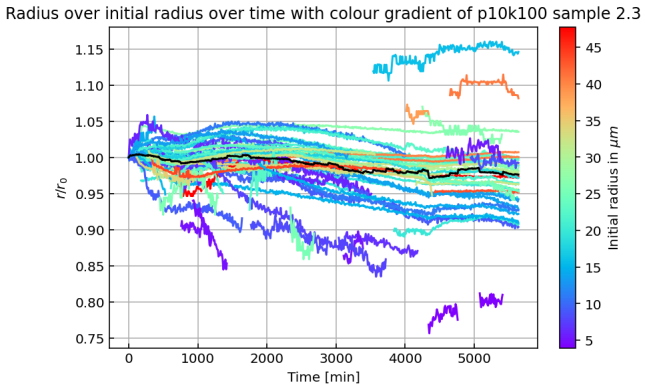

(c)

Figure 4.15: *r/r_0 over time of the P10K100S2 sample with a colour gradient to indicate the initial radius. (a) Well 1. (b) Well 2. (c) Well 3.*

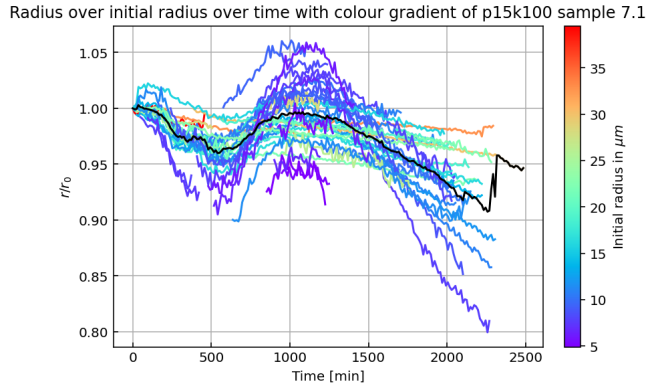

(a)

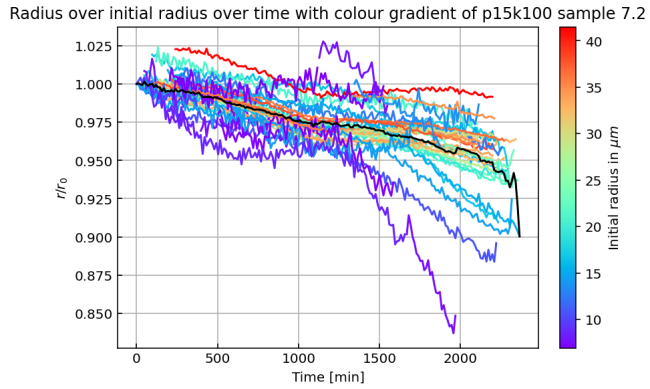

(b)

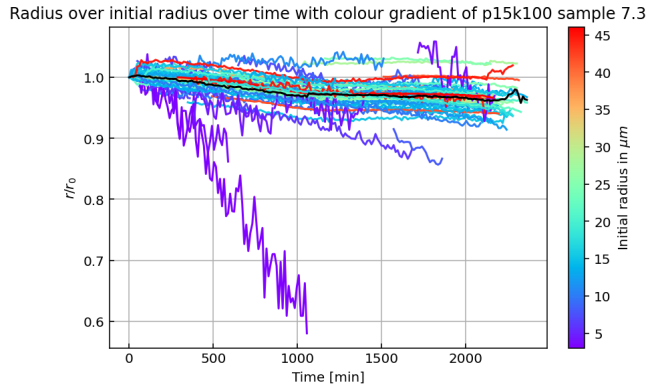

(c)

Figure 4.16: *r/r_0 over time of the P15K100S7 sample with a colour gradient to indicate the initial radius. (a) Well 1. (b) Well 2. (c) Well 3.*

4.7 PLL-g-PEG coating

The PLL-g-PEG method, described in section 3.1, was used for these measurements. Since the droplets do not move using this method the field of view was set to be much bigger, so more data can be gathered during a single measurement. This was done by selecting a smaller region of interest and pasting multiple of these tiles together in a grid with a 15% overlap.

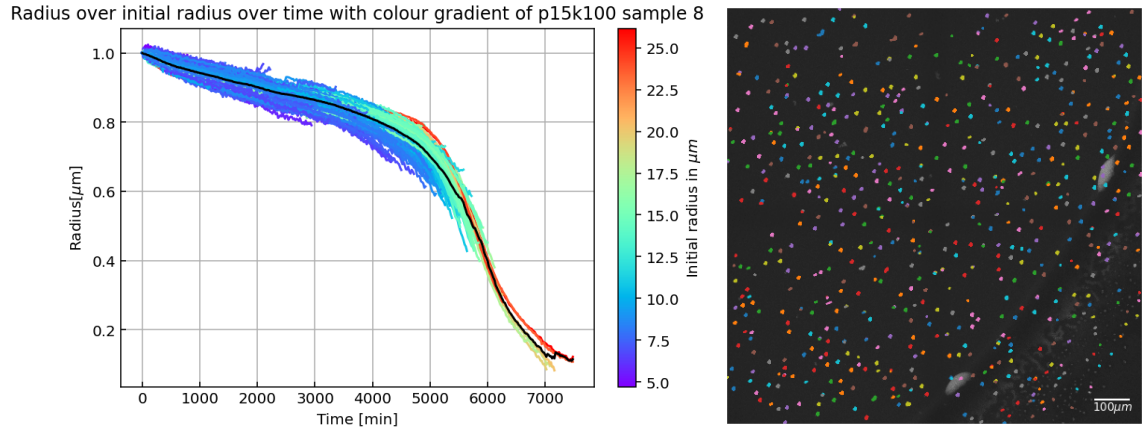

(a) ***(b)***

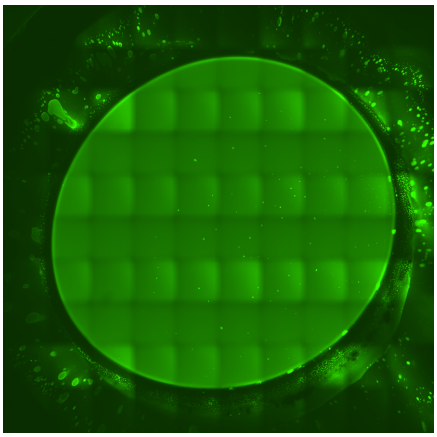

(c)

Figure 4.17: *P15K100S8 data. (a) The r/r_0 over time with a colour gradient to indicate the initial radius. (b) The tracks found by trackpy shown on top of the last frame. (c) The image taken shortly after the measurement concluded. A 10x10 grid was used to get the whole sample in frame.*

The first measurement with this method was a P15K100 sample, listed as P15K100S8, that used $3\mu l$ of sample solution. The measurement ran

for 137 hours with a z-stack every 20 minutes using a 2x2 grid. Figure 4.17 shows the results of the analysis and the tracks found by trackpy. An image was taken after the measurement to see how much the solution evaporated, shown in figure 4.17c. By tracing the contour of the remainder and the faint outline of the area the solution initially covered and letting ImageJ calculate the areas, the area shrunk by roughly 20%.

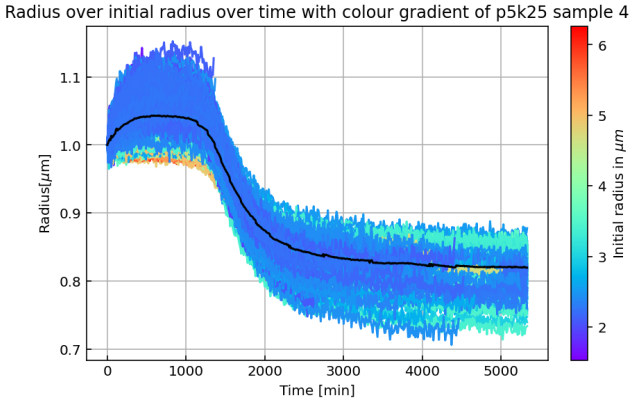

(a)

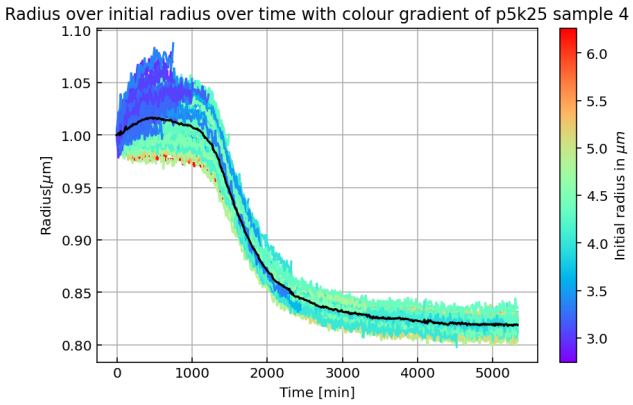

(b)

Figure 4.18: *The r/r_0 over time of the P5K25S4 data with a colour gradient to indicate the initial radius. (a) All droplets. (b) Only droplets larger than $3\mu m$ are shown for visual purposes.*

The second measurement used a P5K25 sample, listed as P5K25S4, with $3\mu l$ of sample solution. This measurement ran for roughly 90 hours with a z-stack every 10 minutes. Due to the small droplet size in this sample, the 40x objective was used with a 5x5 grid to optimise how much data was extracted. The results of the measurement and analysis are shown in

figure 4.18. Figure 4.18b only shows droplets larger than $3\mu m$ for visual purposes.

4.8 General

By plotting just the average ratio of every measurement in one figure, results can be easily compared. Figure 4.19 shows the averages of each measurement with the different sample solutions having their own colour. Do note that these are all the results obtained, meaning they are from different sample types. The wait times (t_w) are also taken into account, so the data in this plot shows the shrinking behaviour from when the sample solution was mixed.

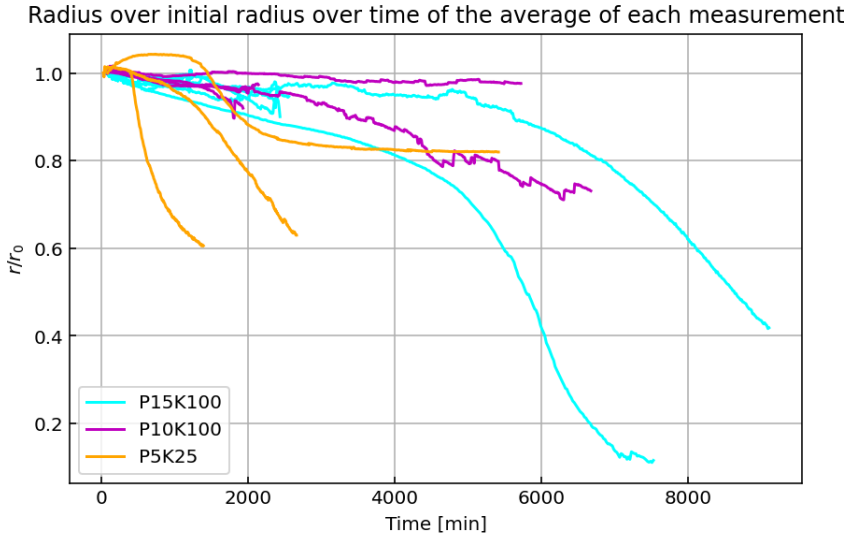

Figure 4.19: *The average ratio of every measurement over time. The colour indicates what sample solution was used for the measurement. Wait times are included.*

An estimate is made for the process of Ostwald ripening. For this the material properties of PGL-3 droplets need to be known. All measurements were taken at room temperature. The surface tension is taken to be $3.5\mu N/m$ [9], the diffusion coefficient to be $0.015\mu m^2/s$ [15]. Putting the protein sequence from the protein stock preparation protocol (figure 7.1) into Protein-Sol yields a solubility of 0.45 [16]. The molar volume is taken to be $0.396m^3/mol$ based on unpublished data from Hubatsch. To make the estimate, the P15K100S8 sample is used since no dropelts enter or leave the frame during the measurement. The average initial radius $R_0 \approx 10.2195\mu m$. Computing and rewriting equation 2.1 gives:

$$\langle R \rangle \approx \sqrt[3]{1.067 \cdot 10^{-15} + 1.4 \cdot 10^{-24} t} \tag{4.1}$$

Consider $t = 60h$, that would yield an $\langle R_{t=60h} \rangle \approx 10.2205 \mu m$. This means a growth in average radius of roughly $0.1nm$. The actual average radius after 60 hours is roughly $9.4529 \mu m$.

Overview of measurements			
Section	Sample	Figures	Purpose
4.1	P15K100S1	4.1, 4.2	Getting a feel for the relevant parameters.
4.2	P15K10021	4.3, 4.4	Investigating effects of imaging on sample.
4.3	P15K100S3	4.5, 4.6	Use longer measurement time to capture shrinking.
4.4	P15K100S4	4.7-4.9	Check whether silicone oil helps seal the wells.
4.5	P15K100S5	4.10	Investigate the cause of the observed drift.
4.6	P5K25S1	4.11, 4.12	See whether multi wells plates are suitable. Gather data at different concentrations.
	P5K25S2	4.13	Gather more data.
	P10K100S1	4.14	Gather data at different concentrations.
	P10K100S2	4.15	Gather more data.
	P15K100S7	4.16	Gather more data.
4.7	P15K100S8	4.17	Gather more data with new coating method.
	P5K25S1	4.18	Gather more data.

Chapter 5

Discussion

In this section the results of both the measurements and their analysis are discussed for each measurement. At the end a short summary is made along with a general discussion, from this the conclusions are made. As a reminder, the naming convention used for the samples follows this example: P15K100 has 15μM PGL-3a and 100mM KCl.

5.1 Reference measurement

The results of the reference measurement show multiple things. Firstly, the identification of the droplets and finding their position and radius works well enough for the purpose of this research. One consideration is to look at the maximum inner circle instead of the minimum enclosing circle, to see if that makes a considerable difference in the found radii of the droplets. This would mean that droplets that just merged, and thus have an elliptical shape, will not be perceived as bigger than they are. On the other hand, using the maximum inner circle could lead to less data being extracted from the frames as the droplet radii would be systematically smaller and could be smaller than the minimum radius threshold. With either method a systematic error is present, overestimating the radii using minimal enclosing circles and underestimating the radii with maximum inner circles. Taking the analysis method into account, with splitting droplets based on a change in radius, the preferred method is the minimum enclosing circle with the benefit of more extracted data.

Next is that the splitting of droplets, where jumps in ratio occur, works as intended but that it can still be optimised. The droplet at the top in figure 4.2b, for example, seems to not have started at a ratio of one, which

it should have. This could be because this droplet has split multiple times before and each previous part was filtered out because these parts were present for shorter lengths than the threshold value. This shows that the filter is not entirely foolproof and that it could be useful to add code that optimises the minimum length and max rate of change filter parameters. For this research it is not worth the time and effort to implement this, but it could be considered for longer projects.

A last and crucial remark is that the droplets do not shrink at this measurement time of roughly one day. For P15K100 samples, longer measurement times could be needed to observe shrinking of droplets. With lower salt concentrations the shrinking is expected to happen sooner, based on earlier observations of the research group, so a measurement time of one day might be enough for those kind of samples. The used frame rate seems to be a good choice for these measurements, although for much longer measurements the size of the data files could become a limiting factor. So a lower frame rate might be necessary for future measurements.

5.2 Control: Imaging

Due to the frame rate of this measurement the limiting factor was storage size. This meant that the measurement was stopped early and thus nothing can be said about the effect of high imaging at timescales longer than used for this result. Setting the frame rate to a similar value as other measurements but without the shutter closing between frames, could show the effects of imaging at longer timescales without the storage limitation.

On the other hand, the droplets did not seem affected by the amount of imaging in this measurement. Considering this measurement already has a much higher frame rate than other measurements will have, the expectation is that with other measurements the effects of imaging are negligible. Other possible influences could be much more impactful on the samples than the effects of imaging, such as evaporation, which is looked at and discussed in sections 4.4 and 5.4 respectively. For this research, the effects of imaging are considered to be negligible.

In figure 4.3b there are multiple droplets that rapidly shrink. By looking at the video file of the raw data it can be explained by droplets moving out of the field of view. The minimum enclosing circle will still try to fit a circle using the part of the droplet that remains in frame. This works with droplets that have their centre still inside the frame, but as soon as the true centre is out of frame, it will fit a new droplet on a new centre with a different radius. These radii get smaller quickly as the droplet keeps moving

out of frame, resulting in the rapidly shrinking droplets in the figure.

The last notable thing is the drift that was mentioned in the results. This drift could cause most of the droplets to leave the frame as the measurement goes on, which means a big loss of data. This could be a big issue if this drift stays present in future measurements.

5.3 Longer timescale

As can be seen in figure 4.5a, shrinking of P15K100 droplets occurs after a longer period of time has passed, compared to the first two measurements. This result is in line with the previous results, where no notable shrinking of P15K100 droplets occurred within a day. It does seem however, that the droplets of this sample did experience slight shrinking within the first day, roughly 5%, where the previous samples did not. This can most likely be attributed to every sample behaving slightly different. It does reinforce the conclusion of imaging not affecting the droplets somewhat, since these droplets did start shrinking while not being subject to strong imaging.

The results also shows that the time needed for future measurements of P15K100 samples would be around 150 hours (6.25 days). This means the measurement time could be a limiting factor in this research, as the amount of gathered data would be limited because of this. For samples with lower salt concentrations, the expected time to measure the same amount of shrinking should be less, as mentioned in section 5.1, which should help with the issue of available time.

A noteworthy find is that it seems that the larger droplets seem to shrink slower, or have a later turnover point than smaller droplets, like McCall noted [13]. This suggests that the initial droplet size is indeed correlated to the shrinking behaviour. However, since only six droplets remain at the end of the measurement, it is impossible to say for sure whether this is the case based on this result. To investigate this, more droplets need to remain in frame throughout the measurement.

The addition of silicone oil around the spacer does not give a clear result whether it prevents evaporation or not. After the measurement, the sample solution evaporated roughly same amount as the previous samples, which did not have silicone oil added, after a similar amount of time. It appeared that the silicone oil ended up between the spacer and the glass slides, thus potentially allowing for more evaporation to take place. This needs to be looked at in more detail to see in what way the silicone oil affects the sample and the results. It is unclear how much this has influenced the results of this measurement. Section 4.4 and 5.4 treat the matter

the silicon oil further.

As can be seen in figure 4.6, the drift is roughly in the same direction as before. Towards the lower right corner of the plots. Again most of the droplets move out of frame during the measurement and data is lost because of this. The drift could be dependent on the sample itself, every sample is different and maybe it is a matter having bad luck with samples with a lot of moving droplets. It could also be that the droplets need to settle first. When the solution is put into the well, the droplets need to descend through the fluid until they rest on the glass slide, this may take some time and this could be the cause of the droplets moving throughout the measurement. A last possibility is that something else makes the droplets move considering the droplets move in roughly the same direction.

5.4 Control: Evaporation

Based on the results it is clear that the addition of silicone oil does not help with evaporation. The silicone oil likely affects the spacer and is able to get between the spacer and the glass slides, breaking the seal on the well. For future glass slide samples, silicone oil will not be used.

The tracks in figure 4.9 again indicate a drift towards the lower right corner of the frame. Meaning that the issue is not droplets that still need to settle, but something else.

Due to the combination of these issues and the resulting data, nothing can be said about the shrinking behaviour of droplets in this sample.

5.5 Control: Drift

Based on the droplets moving towards the lower right corner in both figure 4.10a and 4.10b, it can be said that something is indeed not level, causing the droplets to move in the direction of the lower right corner. After checking the microscope, the floor and the table the microscope was standing on it turned out that the table was not level, causing the drift. This was resolved before the next measurement.

5.6 Multi Well Plates

There is a lot to say about the results from multi well plate measurements.

Starting with the results from the P5K25 measurements. First of all, the difference in droplet size between samples. Why the droplets have such a big difference in size is probably because of the sample preparation. Every sample is slightly different and sometimes the droplets inside the solution are smaller or bigger. If there is a different cause to this, is unknown and not relevant enough for this research.

The need for the 40x objective is due to the droplet size, however, it is unfortunate that the background noise was present, while with the 20x objective it was absent. The cause for the background noise present during that measurement was found by someone else who fixed it. It turned out that the 40x objective was dirty. This issue only affected the P5K25S1 measurement.

Then it should be noted that the droplets do not drift into a set direction anymore, showing that the table was levelled correctly. The amount of movement seen in figure 4.13b is similar to the movement of the rest of the measurements, making the absence of movement in figure 4.12b the outlier. Why this is the case is unknown, it could be because of the smaller droplet size that they stay in place but there is no supporting data for that. In other samples, smaller droplets, with roughly the same size as the droplets in figure 4.13b, move just as much as the bigger ones, for example.

This random movement does mean that the issue with droplets moving into frame, and increasing the average ratio, as can be seen in figure 4.13a, stays present. The code can correctly deal with merging droplets and droplets that leave the field of view, but moving into the field of view is not correctly accounted for.

There is a clear difference in behaviour between the results of the two P5K25 measurements. The P5K25S2 sample shows a similar behaviour to the previous samples, it stays relatively flat and starts shrinking faster after a certain time. This turning point happens at a much earlier time than with P15K100 samples, as previously expected, showing that a lower salt concentration indeed leads to shrinking earlier. However, the P5K25S1 sample shows shrinking droplets immediately, and even more, the shrinking slows down. Because of this, it cannot be said with certainty if the results of either P5K25S1 or P5K25S2 is to be taken as true, more data needs to be gathered.

An interesting thing to note is that larger droplets seem to start shrinking later yet again. See for example figure 4.13a, where, from the droplets that are present at the start, the bigger droplets have a higher ratio than the smaller droplets. If this is the case, it could explain figure 4.12a. The droplets were already small enough that they passed the turning point

before the measurement was even started, thus shrinking rapidly in the beginning. The slowing down of the droplets is not seen elsewhere, but that could be explained by the other measurements being done using a 20x objective. Thus needing a minimum radius in the code for the droplets for trustworthy results and not taking into account the droplets that show this behaviour, as explained in section 3.4.2. It could also be that the behaviour of the droplets in the P5K25S1 sample are an outlier, more data is needed to be sure.

A third P5K25 measurement was done where three wells were recorded at the same tine, but due to a power outage, the datafile was corrupted. The data could be recovered but writing the code had priority and no time was found to restore the datafile within the time limits of the project. It is also unsure if restoring the data would have been worthwhile considering the results of the multi well measurements of the P10K100 and P15K100 samples.

The results of the P10K100 samples do not tell much with certainty. P10K100S1 shows a rather bumpy behaviour of the droplets, for which there is no clear cause. It does, however, seem to show that bigger droplets shrink slower again. From the droplets present at the start, the bigger droplets end with a higher ratio than the smaller droplets. Although it is unconvincing with how little data is present in the figure, again very few droplets remained within the field of view.

The results of P10K100S2 also vary. Well one and two, belonging to figure 4.15a and 4.15b respectively, also have the issue of droplets moving out of frame. So much so, that no droplets remained after a certain point during the measurement. Well three did keep droplets in frame until the end. This did show, again, that every sample behaves differently. While well three did keep droplets in frame, it shows the same bumpy behaviour as P10K100S1 did and no clear shrinking of droplets, even after 5000 minutes (almost 3.5 days). Well two does seem to show clear shrinking behaviour, it does not even cover 2000 minutes. Because of that, it cannot be said for sure that how the P10K100 droplets behave and more data is needed.

Similarly to the results of the P10K100 measurements, the results of the P15K100S7 measurement do not tell much. Well one, corresponding to figure 4.16a, shows a bump in the middle of the measurement. Why this happened is unknown, the other wells do not experience such a bump. None of the wells show clear shrinking behaviour with the exception of a handful of individual droplets. This is in line with the expected time for P15K100 samples, which, based on the results of figure 4.5b, would be around 5000 minutes.

The reason for the droplets moving out of frame in the case of P10K100S2

is unclear, as only two out of three wells end up without any droplets in frame. It seems that it is just unlucky that the droplets moved around so much. Preventing the droplets from moving would greatly improve the amount of data gathered per measurement. This would save time and resources to make samples.

For the P15K100S7 measurement, a large part of the droplets were discarded, between 40% and 50%. This was because the radii of the droplets changed more than the maximum set value and the resulting splits were present for too short to be useful. The cause for this was consecutive merge events with the same droplet and droplets hovering close to the border, which causes issues as explained in section 5.2. The maximum allowed rate of change was the same as for other P15K100 samples, which already should have enough margin to keep most of the droplets. It is unfortunate that this sample had to discard this much data. This could possibly be prevented by droplets not being able to move too, this would eliminate merge events and droplets moving in or out of frame. Which are the causes for having to discard these droplets.

For further measurements the glass slide method will be used as the results from using a multi well plate are too inconsistent in quality. The glass slide method is more consistent, which is preferred over the benefit of doing multiple measurements at a time. It does mean that evaporation needs to be looked at again to get a better idea of how much this affects the samples. A method to prevent droplets from moving has also been tested and found to work by others, this method is described at the end of section 3.1. This method will be used for the next measurements.

5.7 PLL-g-PEG coating

The behaviour in figure 4.17a is very similar to the behaviour in figure 4.5b. The turning point, where droplets start to shrink much faster than before, is also around 5000 minutes in both cases. The only difference being that the P15K100S8 sample shrunk by roughy 25% before the turning point while the P15K100S3 sample only shrunk about 10%. This gives the idea that P15K100 droplets follow this behaviour in general, but this has not been observed every time.

Another remark is that it seems that the bigger droplets, again, seem to start shrinking later than smaller droplets. This behaviour seems to be present in most of the measurements where the droplets behaved consistently.

The P5K25S4 result shows an increase in ratio at the start, the reason

behind this is unsure. However, the smaller droplets grow more than the bigger droplets do. Repeat measurements are needed to check whether this happens every time.

Furthermore, the droplets also slow down in their shrinking. This could be the combined behaviour seen in the figures 4.12a and 4.13a, but that can not be said on this result alone. From this result however, is clear that the P5K25 droplets have their turning point somewhere between 1000 and 1500 minutes. Much earlier than the 5000 minutes of the P15K100 droplets. The question still remains if this is due to salt concentration, droplet sizes, or a combination of both. For this it would be useful to look at more sample solutions.

A last thing to note is evaporation. From the P15K100S8 result in figure 4.17c, roughly 20% of the sample solution evaporated after roughly 140 hours. It does need to be noted that this 20% is an upper bound to the evaporation. While sealing the well during the sample preparation the sample solution would be squished temporarily, this means that the visible outline that was tracked is likely bigger than the actual initial outline of the solution. The edge of the solution is visible in the lower right corner of figure 4.17b and can be seen creeping up in the video file. While this did not create problems for the analysis, it does mean that evaporation cannot be ignored. This much evaporation would mean that the salt concentration goes from $100mM$ to $125mM$ over the course of the measurement. How much this affects the shrinking of droplets should be investigated more. Meca et al. predicts that the samples should still be in the liquid-liquid phase separated regime for the used sample concentrations even if the salt concentration rises because of evaporation [17]. It would be useful to track the evaporation during further measurements to get a better idea of how much changing salt concentrations, and thus evaporation, affects the ageing of the droplets during measurements.

The results of the measurements using this method are the most consistent with how the individual droplets behave from the tried methods. The droplets in both samples follow the averages quite well. This method proves good enough for the type of measurements needed, in combination with the code it works sufficiently to get clear results. If the evaporation can be accounted for, or can be eliminated, the results can be quantified much easier.

The third measurement that was performed, a P10K100 sample, could not be processed and analysed, due to a water leakage in the building that shut down electricity. On top of that, the whole floor was closed off for weeks towards the end of the project, taking away the last possibilities to perform more measurements. This is rather unfortunate, as the sample

preparation method and code were finally developed to a point where they gather and process data efficiently.

5.8 General

Here the overall results are discussed. Firstly the types of samples that were used. Every sample behaves differently and thus it is difficult to find a method that delivers very consistent results. The results from the multi well plates are very inconsistent so the best type of sample is the glass slide sample. From the two tried glass slide methods (PEG-silane and PLL-g-PEG) the PLL-g-PEG coating method is better since the droplets stay in place, meaning that almost no data is lost. The only possible issue with this is the evaporation, but this might not be much in general and this is present for both glass slide methods. It is unfortunate that only one sample can be looked at at a time, but with the large image setting almost the whole sample could be observed, meaning a lot of data is gathered per sample. For measurements with a similar goal, the PLL-g-PEG coated samples are sufficient.

The evaporation is mostly discussed in its own section, it comes down to checking again how much solution evaporates and how much the concentrations change as a result. It could be that the effects are small enough to be ignored, but finding a way to make samples where less evaporation occurs would be useful anyway as this could be of use for other measurements where changing conditions are more bothersome.

The code, in combination with the droplets being stuck in place with the PLL-g-PEG coating, works for the identifying and tracking of droplets and their radii. The main issues within the code are accounting for droplets that move into the frame and droplets that hover near the edge. Having the droplets stuck in place solves this and also means an improved accuracy from trackpy. Incorrect linking was one of the bigger concerns in the code when the droplets moved around a lot. This code can be used in general for tracking multiple droplets where merge events can take place. It can be optimised or adjusted to what is needed.

Now the results, figure 4.19 shows that lower salt concentrations do indeed lead to earlier shrinking. If the protein concentration also plays a role this is unsure, the P10K100 data does not seem to behave differently than the P15K100 data. It would have been great to have more data about other concentrations with the PLL-g-PEG samples so investigate this, but time did not allow for this.

Another thing is the different shrink rates for different initial sizes. Big-

ger droplets do initially shrink slower than small ones, this behaviour shows up in every reliable measurement. It should also be noted that from the P5K25 results in figure 4.19, the two results that had smaller initial droplet sizes ($5\mu m$ instead of $25\mu m$ as the biggest droplets in the 20x samples) and used the 40x objectives show that the shrinking slows down instead of speeding up after a certain point. This could also be relevant to the shrinking behaviour and is already discussed in the previous sections.

The different shrink rates can not be explained by Ostwald ripening alone as can be seen in the estimate. A value of $0.1nm$ is negligible on the scale of the droplets. It might be possible that Ostwald ripening does occur at a relevant scale but is not visible due to the overall shrinking of the droplets, masking the ripening. Should this be the case, it would be possible to check again if Ostwald ripening is relevant. Another thing to note is that Ostwald ripening depends on the material properties of the droplets, but those change as the droplets age. Meaning that the effect of Ostwald ripening would also be age dependent. For now, Ostwald ripening seems to be irrelevant for the shrinking behaviour of the protein droplets and the difference in initial shrink rates is due to something else.

Looking at the volume of the droplets or a ratio of volume and surface area does not reveal anything convincing or new compared to looking at the ratios. It does not show why bigger droplets initially shrink slower for example. There might be something worth investigating when the roundness of the droplets is taken into account. The bigger droplets are slightly flattened due to gravity and this skews the relation between radius and volume a little. However, the droplets seem to be spherical enough for them to be treated that way in the analysis.

A last thing is to look at how the data compares to other results. Looking at data from Nathan, where the diffusion coefficient is plotted logarithmically over time, the ratios found here roughly match the data of the diffusion coefficient. This suggests that there is some relation between the two or that both are caused by some other driving factor.

Chapter 6

Conclusion and outlook

From the discussions a few things can be concluded. First and foremost is that the droplets do indeed shrink at different rates for different salt concentrations, the higher the salt concentration, the slower the shrinking. As far as tested, the shrinking behaviour aligns with the behaviour of other properties of the droplets during the ageing process, leading to the conclusion that the shrinking of droplets is related to the ageing process. In what way the shrinking is related to the ageing remains unsure.

It is also found that larger droplets have a lower initial shrink rate than small droplets, regardless of the concentrations in the sample. The reason for this behaviour remains unknown. The estimate made for Ostwald ripening suggests that it plays no role in this behaviour.

By simply gathering more data at different concentrations using the PLL-g-PEG coated slide method, a more clear picture of the influence of the salt concentration should appear and the shrinking behaviour could be quantified. The same goes for a possible influence of the protein concentration. More data could also shed light on why larger droplets shrink slower than smaller droplets.

A possible theory on what causes the shrinking (and ageing) of droplets will be shown below; this theory would also explain why large droplets shrink slower than small ones. However, every part of the theory is just speculation. It is possible that for some parts there are already some results against or in favour of this theory, but those were not encountered during the project.

The main speculation is that the individual proteins inside a droplet get tangled and eventually form a network that grows from the inside. This tangling would start as soon as phase separation occurs. The next

assumption is that the network stiffens as it grows, since the entangled proteins have less freedom to move. This would explain the increasing viscosity over time. Then it is assumed that the density increases. This would be because the entangled proteins take up less space compared to untangled proteins, meaning that the formation of the network would lead to a higher density. Now the next step assumes that the droplet loses molecules over time, or at least does not have a net gain, this could be due to diffusion. The proteins at the border of the droplet are less connected and could disconnect into the dilute phase. However, since the droplet behaves like a liquid, it has a surface tension, meaning this loss of molecules would be small. Having an increasing density from the forming network and no gain in number of molecules at best means the droplet shrinks. This would be what is observed.

The difference between shrink rate and size could also be explained by this. Suppose the networks form at the same rates regardless of size, the small droplet would experience relatively more shrinking than the large droplet in a certain amount of time. Then it is possible that the rate at which the network would grow starts small (small networks form throughout the droplet), then quickly rises (the individual networks, while still growing, connect into one big network) and slows down again (the last parts of the droplet get entangled). This could explain the increase in shrink rate that is observed and also why the shrink rate decreases for small droplets, since those would mostly have been observed in the last phase.

Assuming that the shrinking due to the diffusing is proportional to the surface area, big droplets should shrink faster than small ones, but this diffusion rate could be low enough that it is not noticeable over the shrinking due to the network forming. After the whole droplet would be entangled, it should still diffuse slowly eventually dissolve completely.

A further speculation is that salt concentration affects how likely the proteins are to connect and tangle, thus affecting how quickly a network would form and the droplet would shrink. Similarly it would dictate how likely proteins are to diffuse into the dilute phase.

Finally, the overall shrinking behaviour of droplets could take the shape of a mirrored sigmoid function, where the derivative (the shrink rate) would match the described rate at which the networks form.

For further research a number of experiments can be done. The first would be to simply perform more measurements like in this research but with different salt and protein concentrations. This could shed light more light on how the salt and protein concentrations affect the shrinking. With more data the effect can be quantified and compared to a mirrored sigmoid

function. To theory can also be tested by: checking whether the proteins would tangle and form a network and if this would increase the viscosity, measuring the density increases over time and tracking the protein concentration in the dilute phase to see if how much protein the droplets lose to diffusion (for this the evaporation needs to be taken into account).

Chapter 7

Appendix

In the appendix the functions of the code (section 7.1), the data parameters (section 7.2) and the protocols (section 7.3) can be found.

7.1 Code

The code developed during this research project is shown below. Only the created functions are shown. The order these functions are used is by first calling the FindCircleData function on the imported datafile. The resulting dataframe is linked using trackpy. After this the ratio r/r_0 is calculated. Then the filters are applied, first the length filter, then the rate of change filter and then the length filter again. This double length filter seems to be the fastest way to filter the data. After the rate of change filter the Reform function is called to put the droplet objects into a dataframe. After the second length filter the Delete function is used to remove droplets that moved into frame. After this the data is plotted.

```
def PrepareData(image):
    # Prepares data with a Gaussian blur and then thresholds the
    data
    blur = cv2.GaussianBlur(image, ksize=(5,5), sigmaX=0, sigmaY=0)
    ret,threshold = cv2.threshold(blur,0,255,cv2.THRESH_BINARY+
    cv2.THRESH_OTSU)
    return threshold

def FindContours(image):
    # Finds contours in image and sorts them by area (largest first)
    image8 = (image*255).astype(np.uint8)
```

```
    contours, _ = cv2.findContours(image8, cv2.RETR_LIST,
    cv2.CHAIN_APPROX_SIMPLE)
    contours = list(contours)
    contours = sorted(contours, key=cv2.contourArea, reverse=True)
    return contours

def FindCircleData(data, min_rad):
    # Creates a dataframe with all circles found (with a radius
    larger than min_rad)
    # and stores their centers, radii, and frame number. Input
    is the imported datafile.
    x = []
    y = []
    radii = []
    frame = []

    for frames in (range(0,len(data)): # stuff per frame
        prepped = PrepareData(data[frames]) # blur and threshold
        data per frame
        contours = FindContours(prepped) # find contours per frame
        for number in range(0, len(contours)): # find data per circle
            circle = cv2.minEnclosingCircle(contours[number]) # fits
            circle for each contour
            xc = (circle[0][0])
            yc = (circle[0][1])
            radius = circle[1]
            if radius > min_rad:
                x.append(xc)
                y.append(yc)
                radii.append(radius)
                frame.append(frames)
            else:
                pass

    df_data = [y, x, radii, frame]
    a = np.asarray(df_data)
    b = np.ndarray.transpose(a)
    df = pd.DataFrame(data = b, columns=['y', 'x', 'radius', 'frame'])
    return(df)

#-------------------------------------------------
```

```
class droplet():
    """
    Droplets from a dataset:
    - number: droplet number given by trackpy as integer
    - X: array of x values of the centre of the droplet
    - Y: array of y values of the centre of the droplet
    - radius: array of radius values of the droplet
    - frames: array of the frames in which the droplet is present
    - roverr: array of radius over initial radius values of the droplet
    Data from arrays with the same index belong to the same frame
    (i.e. droplet x has radius x.r[6] in frame x.f[6])
    """
    def __init__(self, number, X, Y, radius, frames, roverr):
        self.number = number
        self.x = X
        self.y = Y
        self.r = radius
        self.f = frames
        self.roverr = roverr
        self.becomes = number # Gives particle number that comes
        from the split

    def setDroplet(self, number, X, Y, radius, frames, roverr):
        self.number = number
        self.x = X
        self.y = Y
        self.r = radius
        self.f = frames
        self.roverr = roverr
    def setN(self, number):
        self.number = number
    def setX(self, X):
        self.x = X
    def setY(self, Y):
        self.y = Y
    def setR(self, radius):
        self.r = radius
    def setF(self, frames):
        self.f = frames
    def setB(self, become):
        self.becomes = become
```

```
    def setRoverr(self, roverr):
        self.roverr = roverr

#-------------------------------------------------
def CreateDroplet(dataframe):
    # Create object for every droplet from dataframe input
    n = max(dataframe['particle'])
    groups_particles = dataframe.groupby('particle')
    particle_list = [0]*(n+1)
    for particle, group in tqdm(groups_particles):
        x = np.asarray(dataframe['x'][dataframe['particle']
        == particle])
        # Gives array of x data
        y = np.asarray(dataframe['y'][dataframe['particle']
        == particle])
        radius = np.asarray(dataframe['radius'][dataframe
        ['particle'] == particle])
        frames = np.asarray(dataframe['frame'][dataframe
        ['particle'] == particle])
        roverr0 = np.asarray(dataframe['r over r'][dataframe
        ['particle'] == particle])
        part = droplet(particle, x, y, radius, frames, roverr0)
        particle_list[particle] = part
        #particle_list.append(part)
    return particle_list

def Split(drop, numb, frame):
    # Splits droplet object data at a given frame into a new
    droplet and updates
    # the input/old droplet. Depending on conditions this is
    handled differently.
    # Numb is the index the new droplet will receive so it can
    be identified.
    # Frame input is first frame of new droplet.

    index = np.where(drop.f == frame)[0]
    splitx = np.array_split(drop.x, index)
    splity = np.array_split(drop.y, index)
    splitr = np.array_split(drop.r, index)
    splitf = np.array_split(drop.f, index)
    splitroverr = np.array_split(drop.roverr, index)
```

```
    if len(splitroverr[0]) <= 1:
        new_drop = droplet(-numb, [], [], [], [], [])
        drop.setDroplet(drop.number, splitx[1], splity[1], splitr[1],
        splitf[1], splitroverr[1]*splitroverr[0][-1]/splitroverr[1][0])

    elif len(splitroverr[1]) <= 1:
        new_drop = droplet(-numb, [], [], [], [], [])
        drop.setDroplet(drop.number, splitx[0], splity[0], splitr[0],
        splitf[0], splitroverr[0])
    else:
        drop.setDroplet(drop.number, splitx[1], splity[1], splitr[1],
        splitf[1], splitroverr[1]*splitroverr[0][-1]/splitroverr[1][0])
        new_drop = droplet(numb, splitx[0], splity[0], splitr[0],
        splitf[0], splitroverr[0])
    return drop, new_drop

def Reduce(data):
    # Removes empty lists
    less = functools.reduce(operator.iconcat, data, [])
    return less

def Reform(data):
    # Reforms the droplet objects into a dataframe
    # Input is a list with objects and integers
    xdata = []
    ydata = []
    rdata = []
    fdata = []
    pdata = []
    roverrdata = []
    for i in range(len(data)):
        if (type(data[i]) == int) == True: continue
        xdata.append(data[i].x)
        ydata.append(data[i].y)
        rdata.append(data[i].r)
        fdata.append(data[i].f)
        roverrdata.append(data[i].roverr)
        lijst = [i]*len(data[i].f)
        pdata.append(lijst)
```

```
    all_data = [Reduce(ydata),Reduce(xdata),Reduce(rdata),
    Reduce(fdata),Reduce(pdata),Reduce(roverrdata)]
    inv_alldata = list(map(list, zip(*all_data)))
    pdf = pd.DataFrame(inv_alldata, columns=['y', 'x', 'radius',
    'frame', 'particle', 'r over r'])
    return pdf

def RoverR(dataframe):
    # Creates a new column with r/r_0 data
    groups_particles = dataframe.groupby('particle')
    for particle, group in tqdm(groups_particles):
        # Gives int of the last frame a droplet is in
        first_frame = np.min(dataframe.loc[(dataframe['particle']
        == particle)]['frame'].to_numpy())
        # Gives radius of the droplets in their last frame
        r_f = dataframe.loc[(dataframe['particle'] == particle)
        & (dataframe['frame'] == first_frame)]['radius'].to_numpy()
        # Creates new column with r/r_1 in the dataframe
        dataframe.loc[dataframe['particle'] == particle,
        'r over r'] = dataframe.loc[dataframe['particle']
        == particle, 'radius']/r_f[0]
    return dataframe

def LengthFilter(dataframe, length):
    # Drop particles that are present in less than length frames
    groups_particles = dataframe.groupby('particle')
    #dataframe['r over r'] = pd.Series(dtype='float')
    for particle, group in tqdm(groups_particles):
        frame = np.asarray(dataframe.loc[(dataframe['particle']
        == particle)]['frame'].to_numpy())
        if len(frame) < length:
            dataframe = dataframe.drop(groups_particles.
            get_group(particle).index)
        else:
            continue
    return dataframe

def ROCFilter(dataframe, ROC):
    # Takes a dataframe and splits droplets based on the change
    # in radius between frames, anytime a radius changes by more
    # than the value of roc the droplet is split.
```

```
    # 0.05 means 5% change at most is allowed.
    particles = CreateDroplet(dataframe)
    groups_part = dataframe.groupby('particle')
    num = dataframe['particle'].max()+1 # Gives new droplets a
    unique number for identification
    for particle, group in tqdm(groups_part):
        frames = np.asarray(dataframe['frame'][dataframe
        ['particle'] == particle])
        r = np.asarray(dataframe.loc[(dataframe['particle']
        == particle)]['radius'].to_numpy())
        roc = np.diff(r)/r[0]
        for i in range(len(roc)):
            if not abs(roc[i]) > ROC: continue
            particle_index = particles[particle].number
            particles[particle_index], new_drop= Split(
            particles[particle_index], num, frames[i+1])
            particles.append(new_drop)
            num += 1
    return particles

def Delete(dataframe):
    # Deletes droplets from dataframe that are not present
    in the first frame
    groups_part = dataframe.groupby('particle')
    for particle, group in tqdm(groups_part):
        first_frame = np.min(dataframe.loc[(dataframe['particle']
        == particle)]['frame'].to_numpy())
        if first_frame != 0:
            dataframe = dataframe.drop(groups_part.get_group(
            particle).index)
        else:
            continue
    return dataframe
```

7.2 Data parameters

Sample name	Obj.	Frame rate (frames/min)	Min. radius (pixels)	Search range (pixels)	Min. length (frames)	ROC (%)	τ_w (min)
P15K100S1	20x	1/5	5	50	25	1.5	50
P15K100S2	20x	6	5	20	120	1.5	72
P15K100S3	20x	1/15	5	60	25	3	108
P15K100S7	20x	1/12	5	75	25	1.5	75
P15K100S8	20x	1/20	5	20	40	1.5	51
P10K100S1	20x	1/10	5	30	25	1.5	78
P10K100S2	20x	1/10	5	60	25	1.5	84
P5K25S1	40x	1/6	3	20	25	3	404
P5K25S2	20x	1/5	3	20	25	3	24
P5K25S4	40x	1/10	3	30	40	3	88

7.3 Protocols

The protocols on how the PGL-3 protein stock is made and how the slides are prepared before they are used in the samples.

V5232 PGL3-EGFP purification with Liru

PPPips (Protein Preps for People)

Author: Martine Ruer
Entry 112/112: V5232 PGL3-EGFP purification with Liru
No tags associated

Created: 31.01.2023 15:59
Last modified: 01.02.2023 10:53

No custom dates added

V5232
TH0790/D2546
TH0790-pSS2B-ShambaSaha-PGL3-TEV-His6-EGFP
MEANKRQIVEVDGIKSYFFPHLAHYLASNDELLVNNIAQANKLAAFVLGATDKRPSNEEIAEMILPNDSSAYVLAAGMDVCLILGDDFRPKFDSGAEKLSQLGQAHDLAPIIDDEKKISMLARK
TKLKKSNDAKILQVLLKVLGAEEAEEKFVELSELSSALDLDFDVYVLAKLLGFASEELQEEIEIIRDNVTDAFEACKPLLKKLMIEGPKIDSVDPFTQLLLTPQEESIEKAVSHIVARFEEASAVEDD
ESLVLKSQLGYQLIFLVVRSLADGKRDASRTIQSLMPSSVRAEVFPGLQRSVFKSAVFLASHIIQVFLGSMKSFEDWAFVGLAEDLESTWRRRAIAELLKKFRISVLEQCFSQPIPLLPQSELNN
ETVIENVNNALQFALWITEFYGSESEKKSLNQLQFLSPKSKNLLVDSFKKFAQGLDSKDHVNRIIESLEKSSSSEPSATAKQTTTSNGPTTVSTAAQVVTVEKMPFSRQTIPCEGTDLANVLN
SAKIIGESVTVAAHDVIPEKLNAEKNDNTPSTASPVQFSSDGWDSPTKSVALPPKISTLEEEQEEDTTITKVSPQPQERTGTAWGSGDATPVPLATPVNEYKVSGFGAAPVASGFGQFASSN
GTSGRGSYGGGRGGDRGGRGAYGGDRGRGGSGDGSRGYRGGDRGGRGSYGEGSRGYQGGRAGFFGGSRGGSSRENLYFQSSAHHHHHHHVMVSKGEELFTGVVPILVELDGDVNGHK
FSVSGEGEGDATYGKLTLKFICTTGKLPVPWPTLVTTLTYGVQCFSRYPDHMKQHDFFKSAMPEGYVQERTIFFKDDGNYKTRAEVKFEGDTLVNRIELKGIDFKEDGNILGHKLEYNYNSH
NVYIMADKQKNGIKVNFKIRHNIEDGSVQLADHYQQNTPIGDGPVLLPDNHYLSTQSALSKDPNEKRDHMVLKEFVTAAGITLGMDELYKGA*
MW = 104.25 kDa
E = 68,760 reduced

2 x 500 ml Sf+ cells (passage P27) were infected on 27/01/2023 at 1 M/ml with 1 % V5232 virus for 72 h
Almost all cells show a high expression (see cell images Bright field vs. green fluorescence at 1 ms exposure)

TH0790-pSS2B Map.png

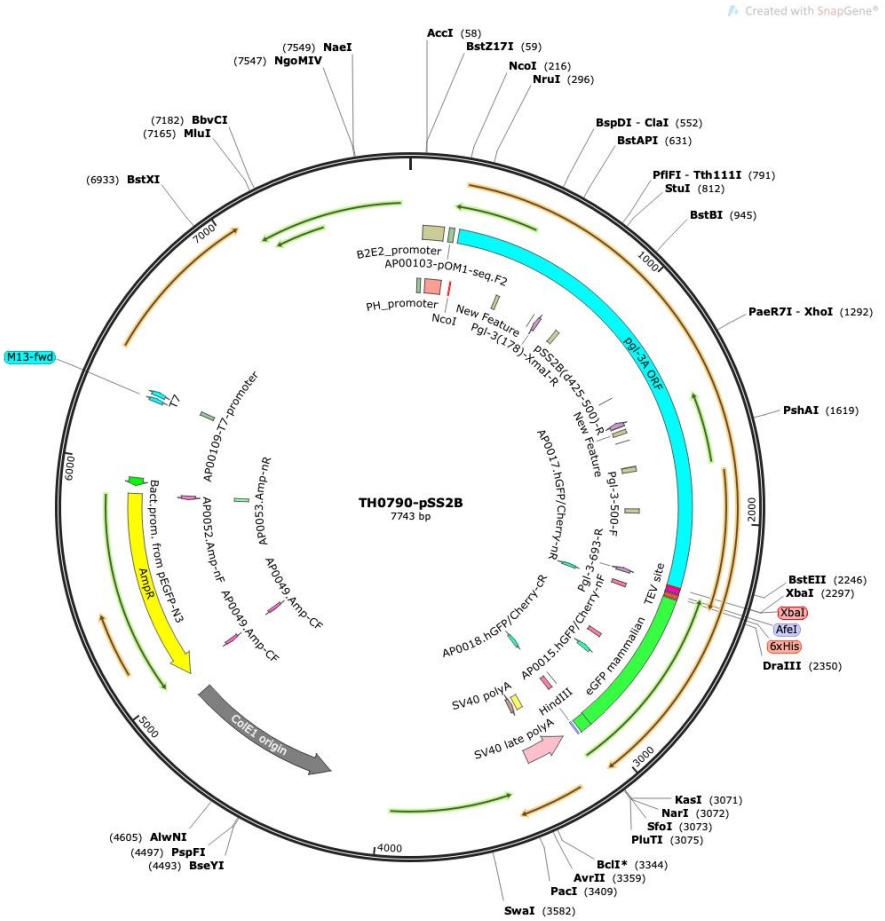

Lysis buffer: 25 mM HEPES pH 7.25, 300 mM KCl, 1 mM DTT, 1 x PIs (1 EDTA-free Roche tablet for 100 ml buffer), 20 mM imidazole
Binding buffer: 25 mM HEPES pH 7.25, 300 mM KCl, 1 mM DTT, 20 mM imidazole
Elution buffer: 18.75 mM HEPES pH 7.25, 225 mM KCl, 1 mM DTT, 250 mM imidazole *(prepare by mixing 3/4 of 25 mM HEPES pH 7.25, 300 mM KCl + 1/4 1 M imidazole pH 8.0)*
Dilution buffer: 25 mM HEPES pH 7.25, 1 mM DTT
HiTrapQ low salt buffer: 25 mM Tris pH 8.0, 50 mM KCl, 1 mM DTT
HiTrapQ high salt buffer: 25 mM Tris pH 8.0, 1 M KCl, 1 mM DTT
Size exclusion buffer: 25 mM HEPES pH 7.25, 300 mM KCl, 1 mM DTT

Cells were collected by centrifugation at 300 rcf for 8 min at RT
Supernatant was discarded
Pelleted cells were resuspended in ~ 60 ml lysis buffer
Cells were lysed using LM20 microfluidizer (2 passes on ice, 12,000 psi)
After lysis, the final volume is ~ 100 ml whole crude lysate
Whole crude lysate was centrifuged in Ti45 rotor at 25,000 rpm for 1 h at 8 °C
Crude supernatant was filtered through a 0.22 µm filter (see picture) (20 µl sample 'CS' for SDS-PAGE)

20230130-PGL3-mGFP-Filtering.jpg

Ni-NTA purification (2 x 2 x 5 ml ProTino columns from Macherey-Nagel, peristaltic pump at RT)
In total, 4 columns
1 column set = 2 columns plugged together
2 column sets = 4 columns in total
Each column set was washed with 25 ml H2O and equilibrated with 25 ml binding buffer
Filtered crude supernatant was loaded on the columns (20 µl sample 'FT' for SDS-PAGE)
Each column set was washed with 100 ml binding buffer (20 µl sample 'WFT' for SDS-PAGE)
Protein was eluted with elution buffer and fractionated in 1.5 ml micro centrifuge tubes
Fractions containing GFP labeled protein were pooled in a 50 ml conical tube to determine the final volume of the pooled fractions (20 µl sample 'HisP' for SDS-PAGE)

Anion exchange chromatography (1 x 5 ml HiTrapQ column, ÅKTA pure 1, RT)
Ni-NTA eluted fractions are in 300 mM KCl. The salt concentration needs to be at 50 mM for binding to the HiTrapQ resin

- Take note of the sample volume

Dilute sample 6 x with dilution buffer
Take note of the total diluted sample volume

- Chromatography was program as such:

- wash column with 5 CV H2O
- 'wake' column with 5 CV HiTrapQ high salt buffer
- equilibrate column with 5 CV HiTrapQ low salt buffer
- load sample on the column, collect the flow-through
- wash column with 5 CV HiTrapQ low salt buffer, collect the flow-through
- elute protein with a 35 CV gradient from 0 % to 50 % HiTrapQ high salt buffer, collect fractions
Protein should elute around 300 mM KCl
- continue gradient over 7 CV from 50 to 100 % HiTrapQ high salt buffer, collect fractions
- wash column with 5 CV HiTrapQ low salt buffer
- wash and store column with 5 CV 20 % EtOH

- After the run, collect 20 µl of the pooled peak fractions was taken for SDS-PAGE

Next time, also take a sample of the flow-through fraction for SDS-PAGE

20230130-PGL3-mGFP-HiTrapQ.jpg

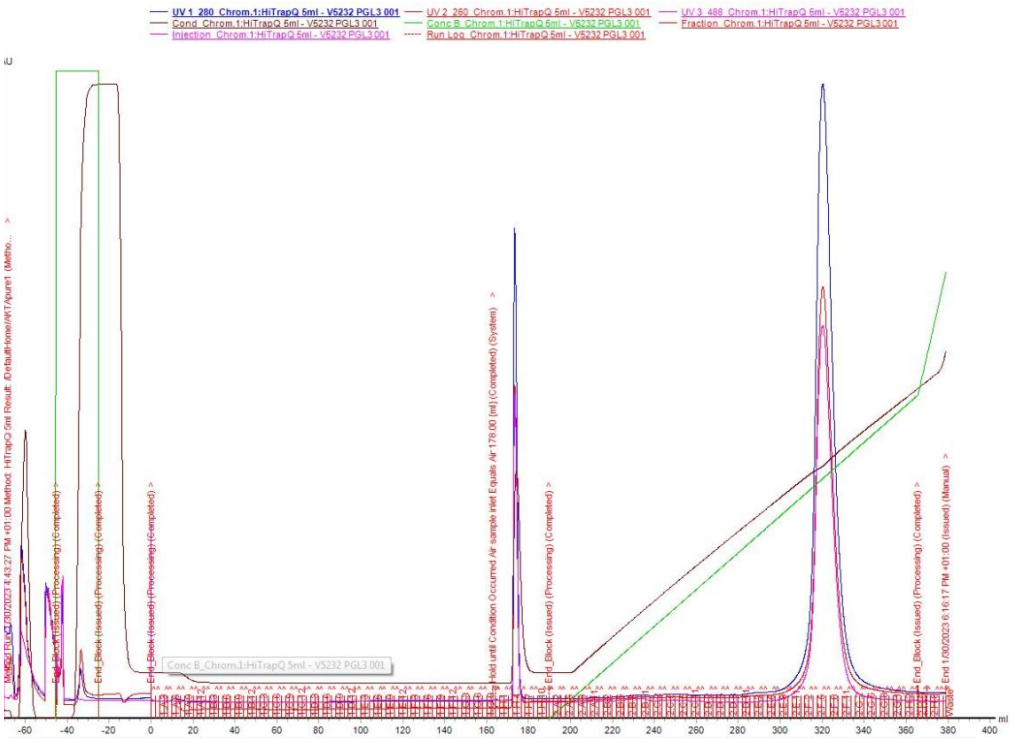

Size exclusion chromatography (Superdex 16/600 200 pg 120 ml Cytiva, ÅKTA pure 1 RT)
Some protein came down in fractions 1H4-1H5. This might be due to some high salt buffer accidentally present in the A1 tubing, although this tubing was thoroughly washed prior to running the method.
We checked if the A260/280 ratio of the protein in these wells was good
A260/280 1H4 = 0.644 √
This ratio matches the requirements for a good quality = low nucleic acid contamination
Peak fraction 2F2 to 2F10 + 1H4 to 1H5 were pooled and concentrated using Amicon 15 ml 30 kDa MWCO down to 5 ml
The sample was filtered through 0.22 µm prior to injecting on the Superdex column
As this sample was very concentrated, the elution peak from the Superdex was very broad
Fractions were loaded to a SDS-PAGE prior to deciding which fractions to pool as the final sample

SDS-PAGE
20 µl sample was mixed with 6 µl 4 x sample buffer
samples were heated at 95 °C for ~ 3 min and centrifuged
supernatant was loaded

Sample concentration and aliquoting
Fractions containing protein (1B7 - 1C7) were pooled and concentrated using 2 x Amicon 15 ml 30 kDa MWCO down to ~ 2 ml
Protein concentration was determined with Nanodrop using the following parameters MW = 104,250 Da; E = 68,760
[PGL3-TEV-His6-EGFP] = 10.83 mg/ml -> 103.9 µM
$A_{260/280}$ = 0.663
Protein was aliquoted in 20 µl fractions in PCR tubes, snap frozen and stored in #49/3

20230131-PGL3-mGFP-SEC.jpg

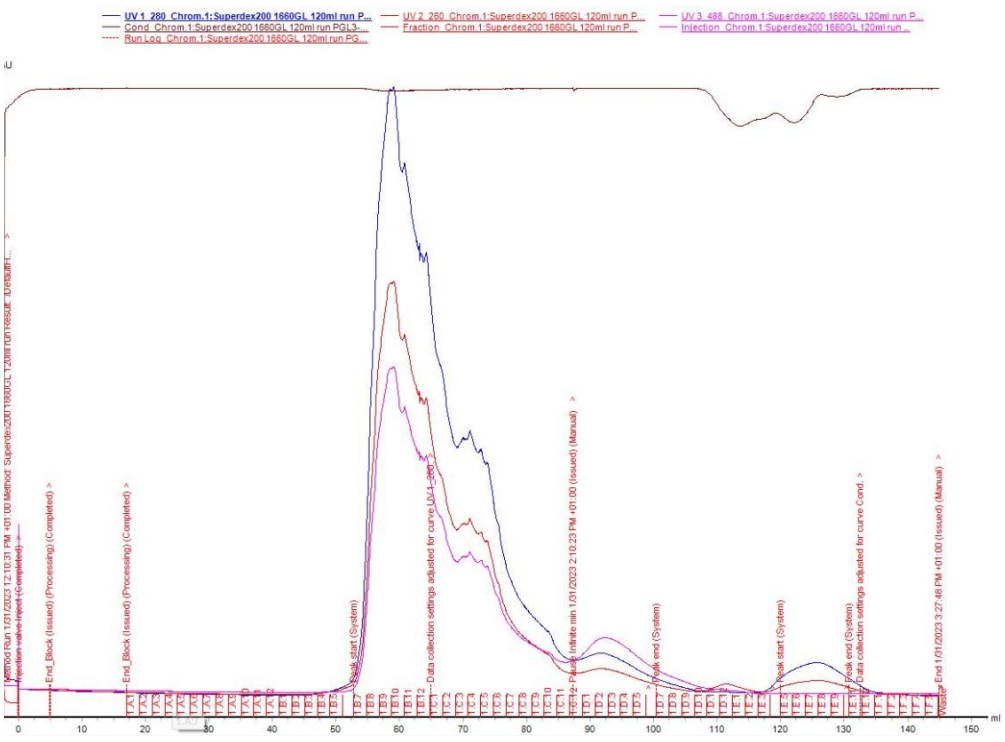

20230131-PGL3-EGFP-FinalProduct-Nanodrop.jpg

Implen NanoPhotometer®

Instrument Type	NP80
Version	NPOS 4.2g build 14900
Serial Number	T81530
Selftest passed	2023-01-27; 17:15
Date	2023-01-31
Time	17:53:38

Parameter

Method	Protein UV	Mol.Ext.Coeff.(1/M*cm)	68760
Type	MolExtCoefficient	Wavelength (nm)	280
Mode	NanoVolume	Background Correction	320 nm
Protein Factor	1.520	Air Bubble Recognition	Off
Volume (ul)	1-2	Manual Dilution Factor	1.000
MW (g/mol)	104250		

#	Name	Conc.	Units	A230	A260	A280	A320	A260/A280	Dilution
1	Blank 1	0.0000	mg/ml	0.000	0.000	0.000	0.000	0.000	
3	Pgl3 1	10.830	mg/ml	40.00	5.163	7.566	0.441	0.663	15

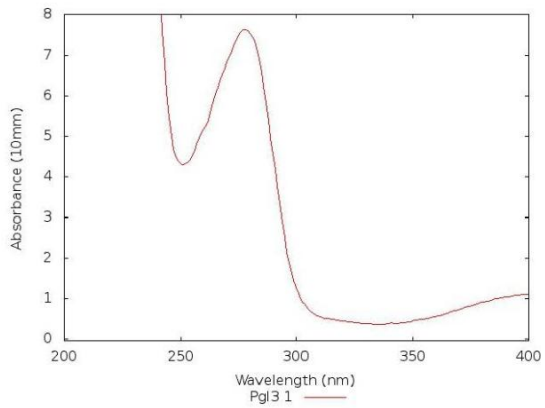

Result 1 / 1 2023-01-31 17:59:04

XLSX Results_2023-01-31_17-59-03
79.5 KB • XLSX

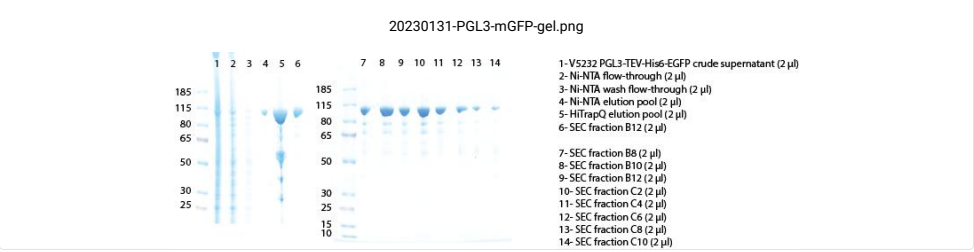

Figure 7.1: *The protocol used for the production of the used PGL-3 protein stock. The protein stock used was prepared by someone else from the research team and had a composition of* $67.5\mu M$ *PGL-3,* $300mM$ *KCl,* $25mM$ *HEPES and* $1mM$ *DTT.*

Awesome PEG – silanization protocol for glass surfaces

July 8, 2017 – Louise Jawerth – Hyman lab

1) Clean Coverslips/glass slides (see note 1)
    a. Put in 2% hellmanex for ~2 hours (see note 1)
    b. Rinse with DiH20
    c. Dry –with compressed air

2) React PEG (see notes 3 & 4)
    a. Measure out 500mL toluene
    b. Add 2300mg PEG silane (or with p~1mg/ml add 2.3 ml of solution) (note 6)
    c. Mix thoroughly so PEG doesn't sink to bottom
    d. Add ~800ul concentrated HCl (36% HCL) (I just eyeball this – so far it has been fine)
    e. Put samples in solution for 18h at RT and stir (cover beaker. Stirring is very important)
3) Cleaning
    a. Rinse samples 1x in Toulene
    b. Rinse samples 2x in Ethanol
    c. Rinse samples 2x in water
    d. Dry with compressed air (or clean house air source)
    e. Store with dessicant (if possible)

Note:

1. On cleaning the coverslips/slides:
    - I have noticed that it still does a decent job of pegylating slides if you just use them straight out the of the box (a relatively clean bunch of slides though) without cleaning them carefully with hellmanex or similar.
    - The main purpose of the hellmanex is to clean your slides and prepare the surface for the silane. If you don't have hellmanex you can plasma treat your slides, dip them in NaOH or use nanostrip/piranha (this is a bit dangerous so look up how to do this safely!) to clean them.
2. The original protocol I used called for half the amount of PEG-silane and HCl. Those slides were good for a while but seemed to "go bad" within a few hours. This protocol seems to be much more robust.
3. I have left my coverslips for several days in step two. This has so far worked out to be fine (make sure you keep stirring).
4. I often reuse the peg-silane solution. When I reuse it, I add new peg-silane and HCl. I usually just reuse it 3-4 times before replacing it with new solution.
5. I also often reuse the rinsing solutions and just replenish them every 4-5 times (except water – that I use fresh every time).

6. PEG silane - I use this one:
    - Cat No. AB111226 from ABCR
    - 3-[Methoxy(polyethyleneoxy)propyl]trimethoxysilane; 90%, 6-9 PE-units
    - https://www.abcr.de/shop/de/catalogsearch/advanced/result/?q=ab+111226
7. Be safe ! Use proper precautions. I do this in the hood and am extra careful with HCl.

Figure 7.2: *The protocol used for the preparation of the PEG-silane coated slides that are used in the samples. This preparation was done by someone else from the research team following this protocol.*

SuSoS
Lagerstrasse 14
1. Stock
CH-8600 Dübendorf
Phone: +41 44 801 80 50
info@susos.com
http://www.susos.com

Material Data Sheet

Chapter 1 – Polymer Details

Product Name (Catalog #)
PLL(20)-g[3.5]-PEG(2)

Chemical Name & Structure
poly(L-lysine)-*graft*-poly(ethylene glycol) co-polymer

Place of Manufacturing
Dübendorf (Switzerland)

Literature

- Elbert, D. L.; Hubbell, J. A. *Chem. Biol.* **1998**, *5*, 177-183.
- Kenausis, G. L.; Voros, J.; Elbert, D. L.; Huang, N. P.; Hofer, R.; Ruiz-Taylor, L.; Textor, M.; Hubbell, J. A.; Spencer, N. D. *J. Phys. Chem. B* **2000**, *104*, 3298-3309.
- Huang, N. P.; Michel, R.; Voros, J.; Textor, M.; Hofer, R.; Rossi, A.; Elbert, D. L.; Hubbell, J. A.; Spencer, N. D. *Langmuir* **2001**, *17*, 489-498.
- Pasche, S.; DePaul, S. M.; Vörös, J.; Spencer, N. D.; Textor, M. *Langmuir* **2003**, *19*, 9216-9225.
- Michel, R.; Pasche, S.; Textor, M.; Castner, D. *Langmuir* **2005**, 21, 12327-12332.
- Morgenthaler, S.; Zink, C.; Städler, B.; Vörös, J.; Lee, S.; Spencer, N. D.; Tosatti, S. G. P. *Biointerphases* **2006**, *1*, 156–165.
- Valentine, M. T.; Fordyce, P. M.; Krzysiak, T. C.; Gilbert, S. P.; Block, S. M. *Nat Cell Biol* **2006**, *8*, 470–476.
- Maddikeri, R. R.; Tosatti, S. G. P.; Schuler, M.; Chessari, S.; Textor, M.; Richards, R. G.; Harris, L. G. *J Biomed Mater Res A* **2008**, *84A*, 425–435.
- Perry, S. S.; Yan, X.; Limpoco, F. T.; Lee, S.; Mueller, M.; Spencer, N. D. *Acs Appl Mater Inter* **2009**, *1*, 1224–1230.
- Lee, S.; Zürcher, S.; Dorcier, A.; Luengo, G. S.; Spencer, N. D. *Acs Appl Mater Inter* **2009**, *1*, 1938–1945.
- Walther, F.; Drobek, T.; Gigler, A. M.; Hennemeyer, M.; Kaiser, M.; Herberg, H.; Shimitsu, T.; Morfill, G. E.; Stark, R. W. *SIA* **2010**.
- Feuz, L.; Jonsson, P.; Jonsson, M. P.; Hook, F. *Acs Nano* **2010**, *4*, 2167–2177.
- Ogaki, R.; Zoffmann Andersen, O.; Jensen, G. V.; Kolind, K.; Kraft, D. C. E.; Pedersen, J. S.; Foss, M. *Biomacromolecules* **2012**, *13*, 3668–3677.

SuSoS
Lagerstrasse 14
1. Stock
CH-8600 Dübendorf
Phone: +41 44 801 80 50
info@susos.com
http://www.susos.com

Specifications
The polymer is composed of a poly(L-lysine) (PLL) backbone to which poly(ethylene-glycol) (PEG) chains are grafted:
- Backbone PLL(bromide): MN = 16'700 – 25'100 g/mol (by SEC-RI-MALS); MW/MN = 1.01 – 1.20 (by SEC-RI-MALS)
- Sidechains -PEG-O-CH_3: MN = 1'800 – 2'200 g/mol (by MALDI); MW/MN ≤ 1.05 (by GPC)
- Target grafting ratio "g" = 3.0 – 4.0

The film is adsorbed from HEPES-1 buffer (pH=7.4) at a polymer concentration of 0.1 mg/mL.

Layer thickness and serum resistance measured by Variable Angle Spectroscopic Ellipsometry on Silicon with natural oxide layer or sputter-coated TiO_2 after aging overnight in HEPES-2 buffer:
- SiO_2 -Typical polymer adsorption: 1.1 – 1.4 nm
  -Serum adsorption less than 0.1 nm
- TiO_2 -Typical polymer adsorption: 0.9 – 1.3 nm
  -Serum adsorption less than 0.1 nm

Package & Storage
Our items carry 12-month validity date after the shipment. They will stay functional for this period or longer if kept at or below -20°C. The shelf life will be significantly shortened if the bottle is opened and recapped frequently, because of introduction of moist and oxygen into the bottle, causing breakdown of PEG side chains and risk of contamination. It is therefore recommended, not to open the bottle multiple times or keep them under an atmosphere of dry nitrogen or argon. Solutions can be stored for 1-2 week time span. During this time they need not to be stored in a freezer. It is better to store them in a refrigerator (4°C) for a short-term storage.

Safety & Handling
This product has not been fully tested yet. Therefore, it is recommended to handle it with all the necessary precaution needed for potentially hazardous chemicals, such as wearing gloves, safety goggles and protective clothing.

Shipping conditions
The samples are shipped at room temperature.

SuSoS
Lagerstrasse 14
1. Stock
CH-8600 Dübendorf
Phone: +41 44 801 80 50
info@susos.com
http://www.susos.com

Chapter 2 – Adsorption Protocol

1 Preparation of PLL-*g*-PEG solution

- Warm up the polymer container to room temperature before opening (reduces condensation of moisture)
- Dissolve the polymer in the appropriate buffer (see buffer details) at a concentration variable between 0.1 and 1.0 mg/mL (depending on application)
- Vortex the solution for a few seconds
- Filter the solution through a 0.2 µm Durapore membrane

2 Substrate cleaning (substrates onto which this or similar polymers have been successfully coated)

- Sonicate the substrates (TiO_2, Nb_2O_5, Ta_2O_5, SiO_2) in 2-propanol for 10 minutes
- Rinse extensively with ultra-pure water
- Dry with a nitrogen stream
- Clean for 2 min with oxygen-plasma

3 Formation of PLL-*g*-PEG monolayer

- Transfer the clean substrates immediately after the oxygen-plasma treatment into the PLL-*g*-PEG solution.
- Incubate the sample at room temperature for 30 minutes.
- Withdraw the sample and rinse it with ultra-pure water and finally dry it under a nitrogen stream
- The samples can be stored in an argon-filled clean glass chamber or directly used for next steps.

Buffer details:

- HEPES-1
  - 10 mM HEPES (4-(2-hydroxyethyl)piperazine-1-ethanesulfonic acid), prepared with ultrapure water (18.3MΩ, TOC<5ppb)
  - Adjusted to pH 7.4 with NaOH or HCl
- HEPES-2
  - 10 mM HEPES (4-(2-hydroxyethyl)piperazine-1-ethanesulfonic acid), prepared with ultrapure water (18.3MΩ, TOC<5ppb)
  - 150 mM NaCl
  - Adjusted to pH 7.4 with NaOH or HCl
- PBS (phosphate ionic strength 10 mM, total ionic strength 150 mM)
  - 8 mM sodium hydrogen phosphate (Na2HPO4.7H2O)
  - 2 mM potassium dihydrogen phosphate (KH2PO4)
  - 3 mM potassium chloride (KCl)
  - 137 mM sodium chloride (NaCl)
  - prepared with ultrapure water (18.3MΩ, TOC<5ppb)
  - Adjusted to pH 7.4 with NaOH or HCl

Figure 7.3: *The protocol used for the preparation of the poly(L-lysine)-graft-poly(ethylene glycol) co-polymer coated slides that are used in the samples. The first step, preparation of PLL-g-PEG solution, was done by Nathan.*

Bibliography

[1] A. A. H. Salman F. Banani, Hyun O. Lee and M. K. Rosen, *Biomolecular condensates: organizers of cellular biochemistry*, NATURE REVIEWS — MOLECULAR CELL BIOLOGY **18**, 285 (2017).

[2] F. W. van Tartwijk and C. F. Kaminski, *Protein Condensation, Cellular Organization, and Spatiotemporal Regulation of Cytoplasmic Properties*, Advanced Biology **6**, 2101328 (2022).

[3] L. Z. e. a. Bin Wang, *Liquid-liquid phase separation in human health and diseases*, Signal Transduction and Targeted Therapy volume **6**, 40 (2021).

[4] Y. Shin and C. P. Brangwynne, *Liquid phase condensation in cell physiology and disease*, Science **357**, 1253 (2017).

[5] L. J. e. a. Avinash Patel, Hyun O. Lee, *A Liquid-to-Solid Phase Transition of the ALS Protein FUS Accelerated by Disease Mutation*, Cell **162**, 1066â (2015).

[6] C. R. E. e. a. Clifford P. Brangwynne, *Germline P Granules Are Liquid Droplets That Localize by Controlled Dissolution/Condensation*, Science **324**, 1729 (2009).

[7] F. J. Anthony A. Hyman, Christoph A. Weber, *Liquid-Liquid Phase Separation in Biology*, Annual Review of Cell and Developmental Biology **30**, 39 (2014).

[8] T. M. Simon Alberti, Amy Gladfelter, *Considerations and Challenges in Studying Liquid-Liquid Phase Separation and Biomolecular Condensates*, Cell **176**, 419 (2019).

[9] M. I. e. a. Louise M. Jawerth, *Salt-Dependent Rheology and Surface Tension of Protein Condensates Using Optical Traps*, Physical Review Letters **121**, 258101 (2018).

[10] S. Biswas and D. A. Potoyan, *Molecular Drivers of Aging in Biomolecular Condensates: Desolvation, Rigidification, and Sticker Lifetimes*, PRX Life **2**, 023011 (2024).

[11] R. Takaki, L. Jawerth, M. Popovic, and F. Julicher, *Theory of Rheology and Aging of Protein Condensates*, PRX Life **1**, 013006 (2023).

[12] L. J. et al., *Protein condensates as aging Maxwell fluids*, Science **370**, 1317 (2020).

[13] K. K. e. a. Patrick M. McCall, *A label-free method for measuring the composition of multicomponent biomolecular condensates*, Nature Nhemistry (2025).

[14] A. BALDAN, *Progress in Ostwald ripening theories and their applications to nickel-base superalloys*, Journal of Materials Science **37**, 2171 (2002).

[15] H. et al., *Quantitative theory for the diffusive dynamics of liquid condensates*, eLife **10**, e68620 (2021).

[16] M. Hebditch, M. A. Carballo-Amador, S. Charonis, R. Curtis, and J. Warwicker, *Protein-Sol: a web tool for predicting protein solubility from sequence*, Bioinformatics **33**, 3098 (2017).

[17] M. E, F. AW, I.-A. JM, R. S, and W. B, *Predicting disordered regions driving phase separation of proteins under variable salt concentration*, Frontiers in Physics **11**, 1213304 (2023).